Journal of Sound and Vibration (1998) **213**(2), 333–374

LIGHT FLUID APPROXIMATION FOR SOUND RADIATION AND DIFFRACTION BY THIN ELASTIC PLATES

D. Habault and P. J. T. Filippi

Laboratoire de Mécanique et d'Acoustique, 31 *chemin Joseph Aiguier*, 13402 *Marseille cedex* 20, *France*

(*Received* 24 *June* 1997, *and in final form* 12 *January* 1998)

This paper deals with the coupling of a thin elastic vibrating plate embedded in a gas. The plate can be baffled or not, or can be part of the boundary of an enclosure. The ratio of the gas density to the plate surface mass is assumed to be small, and thus is a small parameter in the governing equations. The aim of this work is to show that a perturbation method can be used to solve the vibro-acoustics problem. The perturbation method is applied in two different ways. Starting with a boundary integral equation formulation of the problem, the solution is expanded into a Taylor series in the small parameter. In the second approach—which, to our opinion, is newer—the solution is expressed as a series of the resonance modes (free oscillations regimes), and the resonance modes are calculated by a perturbation method. Various examples are proposed.

1. INTRODUCTION

One of the main sources of environmental pollution by noise is the radiation of sound by vibrating structures in contact with air only. This is partly the case in buildings where noise is transmitted through windows, walls or floors: the energy source can be either an incident acoustic wave or a mechanical force which excites the structure directly. Flow noise inside a plane, a car, a high speed train is another example commonly encountered: in these cases, one of the energy sources is the pressure fluctuation induced by the flow (vortex flow or turbulent flow) on the external boundary of the vehicle.

It is well known from experiments that the influence of a surrounding gas on the vibrating regimes of a structure is very small at least away from the resonance frequencies. The main difference between the *in vacuo* behaviour of the structure and its behaviour in a gas occur in the close vicinity of each resonance mode: the difference between an *in vacuo* resonance mode and the corresponding resonance mode of the fluid-loaded structure can hardly be measured, but the resonance frequencies of the fluid-loaded structure are lower than those of the *in vacuo* solid and an extra damping appears which is due to energy loss by sound radiation.

So, in most situations, the influence of a gas on the vibrations of an elastic structure can be considered as a perturbation of the *in vacuo* motion. The asymptotic methods known as *perturbation methods*, which take advantage of the existence of a small parameter—here, the ratio of the gas density to the solid surface mass—are very well suited to such problems. Basically, the solution of the fluid-loaded structure response is sought as a formal Taylor series in the small parameter, which is very often stopped at the first order, the computation of higher order terms being generally very time consuming.

0022–460X/98/220333 + 42 $25.00/0/sv981537

Each term of the perturbation series is obtained by solving two uncoupled problems: the non-homogenous *in vacuo* structure equations and then a non-homogenous Neumann problem for the acoustics equation, the second members of the equations are the solutions of the problem solved at the former step. From a practical point of view, this can be achieved with two independent numerical codes: a program which computes the *in vacuo* response of the vibrating structure, and one which solves the diffraction problem. The coupling between both codes is straightforward.

The validity domain of such approximations is not easy to define. In a preceding paper [1], the authors have considered the response of an infinite fluid-loaded plate to a point force and have given the analytical expression for the first order correcting term. It involves a coefficient proportional to the inverse of the difference between the excitation frequency and the coincidence frequency. This implies that the light fluid approximation cannot be valid in the neighbourhood of the coincidence frequency. For this simple example, the exact solution is known. Thus, the validity domain of a light fluid approximation can easily be defined. It seems quite reasonable to admit that the validity domain of a light fluid approximation is the same for an infinite plate and for a plate with finite dimensions. This provides an *a priori* estimate of the accuracy of the light fluid approximation.

This simple example provides further important information. The space Fourier transform of the fluid-loaded plate response to a point force is readily obtained and can be expanded into a formal Taylor series in the small parameter, the ratio of the fluid density to the plate surface mass. This series appears to be an asymptotic series. This implies that its inverse Fourier transform is an asymptotic series too. Here again, it is reasonable to admit that the perturbation series corresponding to a finite dimension plate is an asymptotic one.

In the examples detailed here, perturbation techniques are developed for two different methods of solution of the governing equations. In the first method, the response of the system elastic structure/fluid is sought as a series of the *resonance modes*—or *free oscillation modes*—of the whole system: these modes are approximated by a small parameter asymptotic technique. In the second method, the boundary value problem is replaced by a system of boundary integral equations which is solved by a perturbation technique.

The first system which is looked at is a thin plate in an infinite perfectly rigid baffle. The excitation force has a harmonic time dependence. The advantage of such a simple configuration is that the development of the leading ideas does not require heavy analytical calculations. Nevertheless, the basic difficulties are clearly pointed out. The comparison between the numerical solution of the exact equations and the *light fluid* approximation, which requires rather simple programming and a relatively short computation time, clearly shows the efficiency of this type of approximation. It must be added that, despite its simplicity, this example provides a good prediction of the insulation index of walls commonly used in the building industry.

The second example is somewhat more complex. It concerns a one-dimensional baffled thin plate (beam) which closes a two-dimensional cavity with perfectly rigid boundaries. The system is excited by the wall pressure exerted by an external turbulent flow. Two kinds of resonance modes are present: the perturbed ones of the *in vacuo* plate modes and the perturbed ones of the rigidly closed cavity modes. If the plate and the cavity have a common resonance frequency, the response of the coupled system is much reinforced. These results are, of course, known and correspond to the intuition which one has of the physical phenomenon; but a perturbation method provides an efficient tool to quantify it. For a random excitation force—here, a turbulent wall pressure is

considered—a second aspect of this vibro-acoustic phenomenon appears: the mechanical system exerts a filtering on the excitation process and the response of the system has high peaks at each resonance frequency which are much increased for common plate/cavity resonance frequencies. Due to its simplicity, this example enables one to study in detail the influence of the various parameters on which the system response depends for a very low computation cost. Furthermore, the physical interpretation of the results is rather easy and can be helpful to understand the behaviour of the response of more complex, though more realistic, systems in which various sub-phenomena can rise together.

The last example deals with the response of a room containing an elastic screen. In room acoustics, screens are commonly used for different purposes. In a factory hall, for example, screens are used to protect workers from the noise radiated by machines. Modern concert halls are commonly equipped with a ceiling having a tunable shape and a movable position: such ceilings are made of light panels. The computer programs used to predict the room performance generally neglect the vibration of the ceiling and, thus, a discrepancy between the predicted response of the room and the experimental one is observed. It is shown here that a perturbation method can easily be implemented in an existing computer code to account for the vibrations of screens.

To prove the existence of a sequence of resonance frequencies and resonance modes is not a classical task. We can cite a paper published in 1989 [2] which deals with the resonances of a three-dimensional elastic solid immersed in a fluid. Using the scattering theory developed in the sixties by P. Lax and R. S. Philips, the authors establish two results: there exists a denumerable sequence of resonance (or free oscillation) modes; they correspond to a set of pairs of resonance frequencies with the same negative imaginary part and real parts of opposite signs. It is reasonable to assume that this result remains valid for the cases studied here which involve thin elastic structures possibly coupled with a cavity.

2. ACOUSTIC RADIATION OF A THIN BAFFLED PLATE

Consider a thin elastic plate occupying the domain Σ of the $z = 0$ plane. The complement Σ' of Σ is perfectly rigid. The boundary of Σ is denoted $\partial\Sigma$; it is assumed that (almost) everywhere a normal unit vector $\mathbf{\check{n}}$, pointing to Σ', can be defined; a tangent unit vector $\mathbf{\check{s}}$ is chosen so that the angle it makes with $\mathbf{\check{n}}$ is positive. The two half-spaces $\Omega^+(z > 0)$ and $\Omega^-(z < 0)$ contain a perfect gas, initially at rest.

The system is excited by harmonic ($e^{-i\omega t}$) sources: S^+ (resp. S^-) are acoustic sources located in Ω^+ (resp. Ω^-) and F is the density of a force acting on the plate. The plate displacement $u(M) = u(x, y)$ is positive when in the $z > 0$ direction. The acoustic pressure in Ω^+ (resp. Ω^-) is $p^+(Q) = p^+(x, y, z)$ (resp. $p^-(Q) = p^-(x, y, z)$). The pressure step across the plate is denoted by $P(M) = P(x, y)$, which is defined by

$$P(x, y) = \lim_{\varepsilon \to 0} [p^+(x, y, \varepsilon) - p^-(x, y, -\varepsilon^-)], \qquad \varepsilon > 0.$$

The acoustic pressure fields $p^+(Q)$ and $p^-(Q)$ satisfy a Helmholtz equation and a Sommerfeld condition at infinity. The plate displacement $u(M)$ obeys a thin plate equation in which the excitation has two terms: the external forces and the pressure step $P(M)$. On the plate, the fluid particle normal accelerations are equal to the plate acceleration. Along the baffle, the pressure fields satisfy homogeneous Neumann conditions. The plate

boundary is characterized by two local boundary conditions. Thus, the functions $u(M)$ and $p^{\pm}(Q)$ are the solutions of the following boundary value problem:

$$
\begin{gathered}
(\Delta + k^2)p^{\pm}(Q) = S^{\pm}((Q)), \qquad Q \in \Omega^{\pm}, \\
(D\Delta^2 - \mu\omega^2)u(M) + P(M) = F(M), \qquad M \in \Sigma, \\
\mathrm{Tr}\ \partial_z p^{\pm}(M) = \omega^2 \mu_0 u(M), \qquad M \in \Sigma, \\
\mathrm{Tr}\ \partial_z p^{\pm}(M) = 0, \qquad M \in \Sigma', \\
\ell u(M) = \ell' u(M) = 0, \qquad M \in \partial\Sigma, \\
\text{Sommerfeld condition for } p^{\pm}
\end{gathered} \tag{1}
$$

The various symbols occurring in these equations are defined as follows: $k^2 = \omega^2/c_0^2$, with c_0 the sound speed in the fluid; μ_0 is the density of the fluid; $\mathrm{Tr}\partial_z p^{\pm}(M) = \lim_{\varepsilon \to 0}[\partial p^{\pm}(x, y, z)/\partial z]_{z=\varepsilon}$, $\varepsilon > 0$ or < 0; $D = Eh^3/12(1 - \nu^2)$; E is Young's modulus of the plate material, ν is its Poisson ratio, h is the plate thickness; μ is the mass of the plate per unit area; ℓ and ℓ' are the boundary operators describing the boundary conditions which the plate displacement satisfies.

In the first step, by using Green's representation of the acoustic pressure this unknown function is eliminated and the boundary value problem is replaced by an integro-differential equation which governs the plate displacement. Then, the eigenmodes and the resonance modes are defined and the representations of the solution as a series of these modes are given. In the third step, a system of boundary integral equations for the plate displacement is established. In the final step, perturbation methods are developed for computing the resonance modes or for solving the system of boundary integral equations. For both representations of the solution, the expressions for the far field asymptotic acoustic pressure are given. The results established here are illustrated by a numerical example.

2.1. Green's representation of the acoustic pressure, integro-differential equation for the plate displacement

This is a very classical task which can be recalled without details. Let $\mathscr{G}_\omega(Q, Q')$ be the Green's kernel which is the solution, in Ω^+, of the Helmholtz equation and which satisfies the Sommerfeld condition at infinity and the homogeneous Neumann condition on the plane $z = 0$. Let $p_0^+(Q)$ (resp. $p_0^-(Q)$) be the acoustic field which is the solution, in Ω^+ (resp. in Ω^-), of the non-homogeneous Neumann problem with S^+ (resp. S^-) as source distribution. The total acoustic fields are given by:

$$
\begin{aligned}
p^+(Q) &= p_0^+(Q) + \omega^2 \mu_0 \int_\Sigma u(M')\mathscr{G}_\omega(Q, M')\, \mathrm{d}\sigma(M'), \qquad Q \in \Omega^+, \\
p^-(Q) &= p_0^-(Q) - \omega^2 \mu_0 \int_\Sigma u(M')\mathscr{G}_\omega(Q, M')\, \mathrm{d}\sigma(M'), \qquad Q \in \Omega^-,
\end{aligned} \tag{2}
$$

This leads to:

$$
P(M) = P_0(M) + 2\omega^2 \mu_0 \int_\Sigma u(M')\mathscr{G}_\omega(M, M')\, \mathrm{d}\sigma(M'),
$$

with

$$P_0(M) = p_0^+(M) - p_0^-(M). \tag{3}$$

Upon using this last relation, the plate equation becomes

$$(D\Delta^2 - \mu\omega^2)u(M) + 2\omega^2\mu_0 \int_\Sigma u(M')\mathscr{G}_\omega(M, M')\,\mathrm{d}\sigma(M') = F(M) - P_0(M) \quad M \in \Sigma,$$

$$\ell u(M) = \ell' u(M) = 0 \quad M \in \partial\Sigma. \tag{4}$$

This is the classical integro-differential equation which governs the displacement of a baffled plate. One also needs to introduce the weak (energetic) form of the equation, which will be helpful for defining the eigenmodes and the resonance modes series representation of the solution. To this end, one can introduce the following bi-linear forms:

$$\langle u, v^* \rangle = \int_\Sigma u v^*\,\mathrm{d}\sigma,$$

$$a(u, v) = D \int_\Sigma \left\{ \Delta u \Delta v^* + (1 - \nu)\left[2\frac{\partial^2 u}{\partial x\,\partial y}\frac{\partial^2 v^*}{\partial x\,\partial y} - \frac{\partial^2 u}{\partial x^2}\frac{\partial^2 v^*}{\partial y^2} - \frac{\partial^2 u}{\partial y^2}\frac{\partial^2 v^*}{\partial x^2} \right] \right\} \mathrm{d}\sigma, \tag{5}$$

$$\beta_\omega(u, v) = \int_\Sigma \int_\Sigma u(M)\mathscr{G}_\omega(M, M')v^*(M')\,\mathrm{d}\sigma(M)\,\mathrm{d}\sigma(M').$$

With v replaced by u, the quadratic form $a(u, u)$ is the bending energy of the plate and $\beta_\omega(u, u)$ is proportional to the energy that the plate loses by acoustic radiation. Then, the plate displacement must satisfy the variational equation

$$a(u, v) - \mu\omega^2 \left\{ \langle u, v \rangle - 2\frac{\mu_0}{\mu}\beta_\omega(u, v) \right\} = \langle F - P_0, v \rangle \ \forall v. \tag{6}$$

The test functions v must be differentiable up to order two, square integrable together with their first and second order derivatives, and they have to satisfy the same boundary conditions as u does. Due to the energy loss in the fluid, there always exists a unique solution for any real frequency.

2.2. EIGENVALUES AND EIGENMODES OF THE FLUID-LOADED PLATE: EIGENMODE SERIES REPRESENTATION OF THE SOLUTION

One can now introduce the coupling parameter $\varepsilon = 2\mu_0/\mu$. The eigenmodes U_n and the eigenvalues Λ_n of operator (6) are defined by

$$a(U_n, v) = \Lambda_n \{ \langle U_n, v \rangle - \varepsilon\beta_\omega(U_n, v) \}. \tag{7}$$

Assume that there exists only one eigenmode for each eigenvalue and introduce $v = U_n^*$ in the former expression. One gets

$$a(U_n, U_m^*) = \Lambda_n \{ \langle U_n, U_m^* \rangle - \varepsilon\beta_\omega(U_n, U_m^*) \}.$$

Use is made of the following symmetry relationships:

$$a(U_n, U_m^*) = a(U_m, U_n^*), \quad \langle U_n, U_m^* \rangle = \langle U_m, U_n^* \rangle, \quad \beta_\omega(U_n, U_m^*) = \beta_\omega(U_m, U_n^*).$$

The first one leads to

$$\Lambda_n \{ \langle U_n, U_m^* \rangle - \varepsilon \beta_\omega(U_n, U_m^*) \} = \Lambda_m \{ \langle U_m, U_n^* \rangle - \varepsilon \beta_\omega(U_m, U_n^*) \}.$$

By using the last two symmetry relationships, an orthogonality relationship between the eigenmodes is obtained:

$$\langle U_n, U_m^* \rangle - \varepsilon \beta_\omega(U_n, U_m^*) = 0 \quad \text{for} \quad m \neq n, \quad \text{or} \quad a(U_n, U_m^*) = 0 \quad \text{for} \quad m \neq n. \tag{8}$$

For eigenvalues of multiple order, the modifications to be introduced are straightforward. A quantity playing the role of a norm can be associated with relationship (8) by

$$a(U_n, U_n^*) = \Lambda_n \{ \langle U_n, U_n^* \rangle - \varepsilon \beta_\omega(U_n, U_n^*) \}. \tag{9}$$

The left side of this equality being real (positive), it is obvious that the Λ_n have non-zero imaginary parts. Furthermore, it must be remarked that the eigenvalues and the eigenmodes depend on the angular frequency ω: this reuslts from the fact that the amount of energy lost by the plate into the fluid is frequency dependent. A similar phenomenon occurs in room acoustics when the impedance of the walls depends on the frequency (see, for example, reference [3]). With each eigenmode U_n, a pressure step P_n and a pressure field p_n are associated:

$$P_n(Q) = 2\omega^2 \mu_0 \int_\Sigma U_n(M') \mathscr{G}_\omega(Q, M') \, \mathrm{d}\sigma(M'), \qquad Q \in \Sigma,$$

$$p_n(Q) = \omega^2 \mu_0 \int_\Sigma U_n(M') \mathscr{G}_\omega(Q, M') \, \mathrm{d}\sigma(M'), \qquad Q \in \Omega^\pm. \tag{10}$$

The plate displacement is now sought as a series of the eigenmodes

$$u(M) = \sum_{n=1}^{\infty} \alpha_n U_n(M),$$

which leads to the variational equation

$$\sum_{n=1}^{\infty} \alpha_n \{ a(U_n, v) - \mu\omega^2 [\langle U_n, v \rangle - \varepsilon \beta_\omega(U_n, v)] \} = \langle F - P_0, v \rangle.$$

By using the orthogonality relationship, it is straightforward to show that the plate displacement is given by the series

$$u(M) = \sum_{n=1}^{\infty} \frac{\Lambda_n}{\Lambda_n - \mu\omega^2} \frac{\langle F - P_0, U_n^* \rangle}{a(U_n, U_n^*)} U_n(M). \tag{11}$$

This series is defined for any real $\mu\omega^2$ because $\Im \Lambda_n \neq 0$, $\forall n$. The pressure fields $p^-(Q)$ and $p^+(Q)$ are expanded into a series of components $p_n(Q)$ as

$$p^\pm(Q) = p_0^\pm(Q) \pm \sum_{n=1}^{\infty} \frac{\Lambda_n}{\Lambda_n - \mu\omega^2} \frac{\langle F - P_0, U_n^* \rangle}{a(U_n, U_n^*)} p_n(Q), \qquad Q \in \Omega^\pm. \tag{12}$$

The main problem is, of course, the determination of the eigenvalues and of the eigenmodes. If the fluid density is small enough, they can be deduced from the *in vacuo* resonance frequencies and resonance modes of the plate.

2.3. RESONANCE FREQUENCIES AND RESONANCE MODES OF THE FLUID-LOADED BAFFLED PLATE: RESONANCE MODES SERIES REPRESENTATION OF THE SOLUTION

The resonance frequencies of the fluid-loaded baffled plate are the frequencies $\omega_n/2\pi$ for which free oscillations are possible. With each of them, a resonance mode w_n (or a finite number of resonance modes) is associated. These modes appear in a natural way when transient regimes are looked at. They satisfy the following boundary value problem:

$$(D\Delta^2 - \mu\omega_n^2)w_n(M)$$

$$+ 2\omega_n^2\mu_0 \int_\Sigma w_n(M')\mathscr{G}_{\omega_n}(M, M')\,\mathrm{d}\sigma(M') = 0, \qquad M\in\Sigma,$$

$$\ell w_n(M) = \ell' w_n(M) = 0, \qquad M\in\partial\Sigma. \tag{13}$$

They are related to the eigenvalues and eigenmodes by

$$w_n = U(\omega_n), \qquad \omega_n^2 = \Lambda_n(\omega_n)/\mu.$$

It is easily shown that if $\omega_n = \tilde{\omega}_n - \mathrm{i}\tau_n$ is a solution, then $\omega_{-n} = -\tilde{\omega}_n - \mathrm{i}\tau_n$ is also a solution.

The resonance modes series representation of the solution is easily deduced from the eigenmodes one. In the first step, the impulse response of the system is calculated by taking the inverse Fourier transform of formulas (11, 12):

$$\tilde{u}(M, t) = \frac{1}{2\pi}\sum_{n=1}^{\infty}\int_{-\infty}^{+\infty}\frac{\Lambda_n}{\Lambda_n - \mu\omega^2}\frac{\langle F - P_0, U_n^*\rangle}{a(U_n, U_n^*)}U_n(M)\,\mathrm{e}^{-\mathrm{i}\omega t}\,\mathrm{d}\omega,$$

$$p^{\pm}(Q, t) = \tilde{p}_0^{\pm}(Q, t) \pm \frac{1}{2\pi}\sum_{n=1}^{\infty}\int_{-\infty}^{+\infty}\frac{\Lambda_n}{\Lambda_n - \mu\omega^2}\frac{\langle F - P_0, U_n^*\rangle}{a(U_n, U_n^*)}p_n(Q)\,\mathrm{e}^{-\mathrm{i}\omega t}\,\mathrm{d}\omega.$$

Because the physical phenomenon must be causal—it cannot start before the sources—it is necessary that the resonance frequencies have a negative imaginary part ($\tau_n > 0$). Thus, the system is at rest for $t < 0$ and, for $t > 0$, its response is

$$\tilde{u}(M, t) = -\mathrm{i}\sum_{n=1}^{\infty}\left\{\frac{\mu\omega_n^2}{\Lambda_n'(\omega_n) - 2\mu\omega_n}\frac{\langle F - P_0, w_n^*\rangle}{a(w_n, w_n^*)}w_n(M)\,\mathrm{e}^{-\mathrm{i}\tilde{\omega}_n t - \tau_n t}\right.$$

$$\left. - \frac{\mu\omega_n^{*2}}{\Lambda_n'^*(\omega_n) - 2\mu\omega_n^*}\frac{\langle F - P_0, w_n^*\rangle^*}{a(w_n, w_n^*)^*}w_n^*(M)\,\mathrm{e}^{-\mathrm{i}\tilde{\omega}_n t - \tau_n t}\right\}, \tag{14}$$

$$\tilde{p}^{\pm}(Q, t) = \tilde{p}_0^{\pm}(Q, t) \mp \mathrm{i}\sum_{n=1}^{\infty}\left\{\frac{\mu\omega_n^2}{\Lambda_n'(\omega_n) - 2\mu\omega_n}\frac{\langle F - P_0, w_n^*\rangle}{a(w_n, w_n^*)}\Psi_n(Q)\,\mathrm{e}^{-\mathrm{i}\tilde{\omega}_n t - \tau_n t}\right.$$

$$\left. - \frac{\mu\omega_n^{*2}}{\Lambda_n'^*(\omega_n) - 2\mu\omega_n^*}\frac{\langle F - P_0, w_n^*\rangle^*}{a(w_n, w_n^*)^*}\Psi_n^*(Q)\,\mathrm{e}^{-\mathrm{i}\tilde{\omega}_n t - \tau_n t}\right\}, \tag{15}$$

$$\Psi_n(Q) = \mu_0 \omega_n^2 \int_\Sigma w_n(M') \mathscr{G}_{\omega_n}(Q, M') \, \mathrm{d}\Sigma(M').$$

It can be remarked that, if the source densities are real functions, then the plate displacement and the sound pressure fields are described by real functions too. The resonance modes series, which represents the time harmonic dependent response of the system, is obtained by taking the Fourier transform of equations (14, 15):

$$u(M) = \mathrm{i} \sum_{n=1}^{\infty} \left\{ \frac{\mu \omega_n^2}{\Lambda_n'(\omega_n) - 2\mu\omega_n} \frac{\langle F - P_0, w_n^* \rangle}{a(w_n, w_n^*)} \frac{w_n(M)}{\mathrm{i}(\omega - \tilde{\omega}_n) - \tau_n} \right.$$

$$\left. - \frac{\mu \omega_n^{*2}}{\Lambda_n'^*(\omega_n) - 2\mu\omega_n^*} \frac{\langle F - P_0, w_n^* \rangle^*}{a(w_n, w_n^*)^*} \frac{w_n^*(M)}{\mathrm{i}(\omega + \tilde{\omega}_n) - \tau_n} \right\}, \tag{16}$$

$$p^{\pm}(Q) = p_0^{\pm}(Q) \pm \mathrm{i} \sum_{n=1}^{\infty} \left\{ \frac{\mu \omega_n^2}{\Lambda_n'(\omega_n) - 2\mu\omega_n} \frac{\langle F - P_0, w_n^* \rangle}{a(w_n, w_n^*)} \frac{\Psi_n(Q)}{\mathrm{i}(\omega - \tilde{\omega}_n) - \tau_n} \right.$$

$$\left. - \frac{\mu \omega_n^{*2}}{\Lambda_n'^*(\omega_n) - 2\mu\omega_n^*} \frac{\langle F - P_0, w_n^* \rangle^*}{a(w_n, w_n^*)^*} \frac{\Psi_n^*(Q)}{\mathrm{i}(\omega + \tilde{\omega}_n) - \tau_n} \right\}. \tag{17}$$

These expressions require the knowledge not only of the resonance frequencies and the resonance modes but also of the derivatives $\Lambda_n'(\omega)$ of the eigenvalues $\Lambda_n(\omega)$ with respect to the angular frequency ω. Perturbation methods allows one to give analytic approximations of these quantities.

2.4. INTEGRAL REPRESENTATION OF THE FLUID-LOADED PLATE DISPLACEMENT: BOUNDARY INTEGRAL EQUATIONS

Modal series are not, in general, the easiest way to solve boundary value problems. Indeed, they are really efficient for simple geometries which allow one to separate the variables. Among all the numerical methods of more or less universal use, boundary element methods have proved to be particularly efficient as far as partial differential equations with constant coefficients are concerned (systems composed of different homogeneous materials). Furthermore, boundary element methods can be used to evaluate numerically the eigenmodes and the resonance modes, and thus provide an efficient tool of general use for the computation of modal series. Finally, the boundary integral equations which describe the oscillations of a structure coupled to a light fluid are amenable to perturbation methods.

An integral representation of the plate displacement is obtained through the *in vacuo* infinite plate Green's kernel which is defined by

$$(D\Delta_M^2 - \mu\omega^2)\gamma(M, M') = \delta_{M'}(M), \qquad M \text{ and } M' \in \mathbf{R}^2$$

(the notation Δ_M^2 means that the derivatives are taken with respect to the co-ordinates of M). The uniqueness of γ is ensured by adding a suitable Sommerfeld condition at infinity. Its expression is classical and will not be recalled here.

An integral representation of the plate displacement takes the form

$$u(M) = \gamma * [F - P_0](M) - 2\omega^2\mu_0 \left(\gamma * \int_\Sigma u \mathscr{G}_\omega \right)(M) + \gamma * [s_1 + s_2](M) \quad \forall M \in \Sigma. \tag{18}$$

In this expression $f * g$ stands for the convolution product of the two distributions f and g. The first two terms are given by

$$\gamma * [F - P_0](M) = \int_\Sigma \gamma(M, M')[F(M') - P_0(M')]\, \mathrm{d}\sigma(M'),$$

$$2\omega^2\mu_0\left(\gamma * \int_\Sigma u\mathscr{G}_\omega\right)(M) = 2\omega^2\mu_0 \int_\Sigma \int_\Sigma \gamma(M, M'')\mathscr{G}_\omega(M'', M')u(M')\, \mathrm{d}\sigma(M')\, \mathrm{d}\sigma(M'').$$

In the third term, s_1 and s_2 are layer sources supported by $\partial\Sigma$ and of different orders (see, for example, reference [4] or [5]): if the Green's representation of the displacement is adopted, the layer source densities have a physical interpretation.

One is left with three unknown functions: the plate displacement $u(M)$ and the densities of the boundary sources s_1 and s_2. The first boundary integral equation is given by equality (18); two others are obtained by writing $u(M)$, as given by (18), satisfies the boundary conditions

$$\ell\left\{\gamma * [F - P_0](M) - 2\omega^2\mu_0\left(\gamma * \int_\Sigma u\mathscr{G}_\omega\right)(M) + \gamma * [s_1 + s_2](M)\right\} = 0,$$

$$\ell'\left\{\gamma * [F - P_0](M) - 2\omega^2\mu_0\left(\gamma * \int_\Sigma u\mathscr{G}_\omega\right)(M) + \gamma * [s_1 + s_2](M)\right\} = 0, \qquad \forall M \in \partial\Sigma. \tag{19}$$

2.5. PERTURBATION METHOD SOLUTION

If the fluid is a gas, its density μ_0 is generally small compared to the surface mass μ of the plate. Accounting for this property, the solution of the equations can be sought as a formal Taylor series of the small parameter μ_0/μ. The choice of this parameter requires some comments.

First of all, it is useful to note that no unit appears in the equations. Thus, the interpretation of the various parameters involved has to be given. For example, h, which stands for the plate thickness, is in fact the ratio of the plate thickness to the unit length which has been omitted in the equations: thus, h is a dimensionless number. The same remark applies for every quantity involved in the problem: in particular, μ_0/μ is the dimensionless number which measures the ratio of the fluid density to the plate surface mass, in a given system of units.

Let $\overline{t}$ and $\overline{\ell}$ be respectively the time unit and the length unit. It is classical to introduce what is commonly called *non-dimensional equations*. To that aim, the following change of units is used: the time unit $\overline{T} = \tilde{T}_c\overline{t}$ is the inverse of the coincidence frequency and one has

$$\tilde{T}_c = 1/f_c = (2\pi/c_0^2)[Eh^3/12(1 - \nu^2)\mu]^{1/2}.$$

The length unit $\lambda_c = \tilde{L}_c\overline{\ell}$ is the wavelength in the fluid at the coincidence frequency:

$$\tilde{L}_c = c_0\tilde{T}_c = (2\pi/c_0)[Eh^3/12(1 - \nu^2)\mu]^{1/2}.$$

It must be noticed that $\tilde{T}_c$ is a dimensionless number which represents the ratio of the new time unit to the initial one; similarly, $\tilde{L}_c$ is a dimensionless number. The governing

equations have exactly the same form as equations (1). Expressed in these new units, the value of the ratio of the fluid density to the plate surface mass is

$$\tilde{\mu}_0/\tilde{\mu} = (\mu_0/\mu)(2\pi/c_0)[Eh^3/12(1-\nu^2)\mu]^{1/2}.$$

In a review article, Crighton [6] has pointed out that this parameter is always small for practical situations, including water/structure interactions. It could be tempting to use a series expansion in terms of this parameter. But, when the series so obtained is written in the initial units, one obtains the series that will be proposed here. As a consequence, the relative errors given by both series are identical.

Nevertheless, the use of this "intrinsic fluid loading unit system" can have some advantages: in particular, the corresponding equations describe a class of physical systems instead of a particular system. But, for the comparison between the behaviours of two different physical systems, it is necessary to adopt the same system of units for both of them. Up to now, no unit system has been specified in this paper: thus, unless the converse is stated, the equations can be considered as written in a classical system of units or in the intrinsic fluid loading unit system as well.

Perturbation techniques have been used for a long time and their efficiency has been proved for a lot of applications. Different presentations of the method that is used in this paper are described in classical books, among them one can cite references [7–9], in the last of which is entitled the *Rayleigh–Schrödinger Method*. A perturbation solution will be established for both approaches of the problem: the eigenmodes series and the boundary integral equations.

This introductory paragraph is concluded by recalling that the light fluid approximation series is not valid around the coincidence frequency: in its neighbourhood, it is certainly possible to find another kind of expansion which can, perhaps, be matched to the light fluid approximation series. It must be added that this paper presents only the lowest order correcting term: indeed, in our opinion, the higher order terms (though their expressions can easily be given) require too much computation effort to be of real practical interest.

2.5.1. *Approximation of the eigenmodes of the system and the eigenmodes series representation of the solution*

Upon introducing the parameter $\varepsilon = 2\mu_0/\mu$, the eigenvalues Λ_n and the eigenmodes U_n can be formally expanded into Taylor series in ε:

$$U_n = U_n^0 + \varepsilon U_n^1 + \varepsilon^2 U_n^2 + \ldots, \qquad \Lambda_n = \Lambda_n^0 + \varepsilon \Lambda_n^1 + \varepsilon^2 \Lambda_n^2 + \ldots.$$

These expansions are introduced into equation (7) and the coefficients of the successive powers of ε are made equal to zero, which leads to a sequence of equations, the zero and first order ones being

$$a(U_n^0, v) = \Lambda_n^0 \langle U_n^0, v \rangle, \tag{20}$$

$$a(U_n^1, v) = \Lambda_n^1 \langle U_n^0, v \rangle - \Lambda_n^0 \beta_\omega(U_n^0, v) + \Lambda_n^0 \langle U_n^1, v \rangle. \tag{21}$$

Equation (20) is for the eigenmodes (or resonance modes) of the *in vacuo* plate. It is assumed that these eigenmodes and the corresponding eigenfrequencies are known (analytically or numerically). By writing equation (21) for $v = U_n^{0*}$, one gets

$$\begin{aligned} a(U_n^1, U_n^{0*}) &= a(U_n^0, U_n^{1*}) \\ &= \Lambda_n^1 \langle U_n^0, U_n^{0*} \rangle - \Lambda_n^0 \beta_\omega(U_n^0, U_n^{0*}) + \Lambda_n^0 \langle U_n^0, U_n^{1*} \rangle. \end{aligned}$$

Equality (20) gives the value of Λ_n^1:

$$\Lambda_n^1 = \Lambda_n^0 \frac{\beta_\omega(U_n^0, U_n^{0*})}{\langle U_n^0, U_n^{0*} \rangle}$$

$$= \Lambda_n^0 \frac{\displaystyle\int_\Sigma \int_\Sigma U_n^0(M)\mathscr{G}_\omega(M, M')U_n^0(M')\,\mathrm{d}\sigma(M)\,\mathrm{d}\sigma(M')}{\displaystyle\int_\Sigma U_n^0(M)^2\,\mathrm{d}\sigma(M)}. \tag{22}$$

Then the first order correction U_n^1 of the eigenmode U_n^0 is expanded into a series of the U_q^0 of the form

$$U_n^1 = \sum_{q=1}^{\infty} \alpha_{nq}^1 U_q^0.$$

Equation (21) is written with $v = U_m^{0*}$ for all m and the orthogonality relationship $a(U_n^0, U_m^{0*}) = \langle U_n^0, U_m^{0*} \rangle = 0$ for $n \neq m$ between the eigenmodes is accounted for. This leads to the equalities

$$\alpha_{nm}^1(\Lambda_m^0 - \Lambda_n^0)\langle U_n^0, U_m^{0*} \rangle = \Lambda_n^0 \beta_\omega(U_n^0, U_m^{0*}) \qquad \forall m \neq n,$$

which uniquely determines the coefficients α_{nm}^1 for $m \neq n$. If $m = n$, an undetermined form is obtained. As suggested in reference [9], one chooses $\alpha_{nm}^1 = 0$: thus, the error in the orthogonality relationship (8) is $\mathcal{O}(\varepsilon^2)$ and the difference between the norms of the functions U_n^0 and $U_n^0 + \varepsilon U_n^1$ is also $\mathcal{O}(\varepsilon^2)$. One finally gets the following result:

$$U_n^1(M) = -\sum_{q=1, q\neq n}^{\infty} \frac{\Lambda_n^0}{\Lambda_q^0 - \Lambda_n^0} \frac{\beta_\omega(U_n^0, U_q^{0*})}{\langle U_q^0, U_q^{0*} \rangle} U_q^0(M)$$

$$= -\sum_{q=1, q\neq n}^{\infty} \frac{\Lambda_n^0}{\Lambda_q^0 - \Lambda_n^0} \frac{\displaystyle\int_\Sigma \int_\Sigma U_n^0(M)\mathscr{G}_\omega(M, M')U_q^0(M')\,\mathrm{d}\sigma(M)\,\mathrm{d}\sigma(M')}{\displaystyle\int_\Sigma U_q^0(M)^2\,\mathrm{d}\sigma(M)} U_q^0(M). \tag{23}$$

This expression involves a double integral over the plate domain Σ. Higher order correcting terms will involve integrations of increasing orders: it seems that such expressions are not interesting from a practical point of view because they rapidly require a very large amount of computation. Our own experience has shown that it is simpler to solve numerically the exact equations rather than to compute the second order approximation. Nevertheless, if an algorithm well adapted to this kind of integral can be developed, the computation of higher order approximations can be more efficient than solving the exact equations.

The first order approximation of the eigenmodes series of the solution takes the following form:

$$u(M) \simeq \sum_{n=1}^{\infty} \frac{\Lambda_n^0 + \varepsilon\Lambda_n^1}{\Lambda_n^0 + \varepsilon\Lambda_n^1 - \mu\omega^2} \frac{\langle F - P_0, U_n^{0*} + \varepsilon U_n^{1*} \rangle}{a(U_n^0 + \varepsilon U_n^1, U_n^{0*} + \varepsilon U_n^{1*})} [U_n^0(M) + \varepsilon U_n^1(M)], \tag{24}$$

$$p^{\pm}(Q) \simeq p_0^{\pm}(Q) \pm \sum_{n=1}^{\infty} \frac{\Lambda_n^0 + \varepsilon \Lambda_n^1}{\Lambda_n^0 + \varepsilon \Lambda_n^1 - \mu\omega^2} \frac{\langle F - P_0,\, U_n^{0*} + \varepsilon U_n^{1*} \rangle}{a(U_n^0 + \varepsilon U_n^1,\, U_n^{0*} + \varepsilon U_n^{1*})} \hat{p}_n(M), \tag{25}$$

with

$$\hat{p}_n(M) = \omega^2 \mu_0 \int_\Sigma [U_n^0(M') + \varepsilon U_n^1] \mathscr{G}_\omega(M, M')\, \mathrm{d}\sigma(M'),$$

which is the first order approximation of $p_n(M)$ as given by equation (10).

The same method provides the approximation of the resonance frequencies and of the resonance modes and lead to the first order approximation of the solution in terms of a series in the resonance modes. Furthermore, the approximation of the resonance frequencies is easily deduced from that of the eigenfrequencies; the approximation of a resonance mode is obtained by replacing the eigenvalue Λ_n by $\mu\omega_n^2$ in the approximate expression of the corresponding eigenmode.

2.5.2. *Perturbation solution of the boundary integral equations*

An approximate solution of equations (18, 19) can be obtained in the same way, by stating that the unknown functions can be expanded into formal Taylor series of the parameter ε. It is immediately found that the zero order equations reduce to the *in vacuo* plate boundary integral equations. These equations have a unique solution if and only if the angular frequency is not a resonance frequency of the *in vacuo* plate.

If the plate material has significant damping, the *in vacuo* resonance frequencies of the plate have a finite imaginary part, and, thus, the *in vacuo* plate equation can be solved for any real frequency. But, if the damping is zero (or very small), due to real (or numerically real) *in vacuo* resonance frequencies, the zero order equations cannot be solved for any real frequency and the perturbation method cannot be applied in a straightforward way. Thus, particular attention must be paid to this case.

To overcome the difficulty presented by the elastic case, an arbitrary damping is introduced into the plate equation as follows:

$$(D\Delta^2 - \mu_1\omega^2)u(M) + \varepsilon\omega^2 \left[\alpha\mu u(M) + \int_\Sigma u(M') \mathscr{G}_\omega(M, M')\, \mathrm{d}\sigma(M') \right]$$

$$= F(M) - P_0(M) \qquad \forall M \in \Sigma, \quad \text{with} \quad \mu_1 = \mu(1 + \varepsilon\alpha), \qquad \Im\alpha \neq 0. \tag{26}$$

The choice of α is *a priori* arbitrary. But it is better that the zero order equation, that is the equation obtained by neglecting the terms multiplied by ε in equation (26), involves a damping factor which is not too far from the one due to the energy radiation into the fluid. The approximate expression for the eigenvalues suggests the following choice. Let $V(M)$ be the *in vacuo* displacement of an infinite plate exicted by a point force. The ratio

$$\tilde{\alpha} = \frac{\displaystyle\int_\Sigma \int_\Sigma V(M) \mathscr{G}_\omega(M, M') V(M')\, \mathrm{d}\sigma(M)\, \mathrm{d}\sigma(M')}{\displaystyle\int_\Sigma V(M)^2\, \mathrm{d}\sigma(M)}$$

leads to the following choice for α: $\alpha = |\Re\tilde{\alpha}| + i|\Im\tilde{\alpha}|$. Other functions $V(M)$ can be adopted, as, for example, the *in vacuo* plate resonance mode, the frequency of which is the closest to the excitation frequency. One can also proceed in two steps. Using the former choice of α, one calculates the response u_0 of the corresponding damped plate and then uses this for a new estimation of α. Our own experience has shown that this method is very efficient and requires very few additional computations.

Let $\gamma_1(M)$ be the elementary kernel of the damped plate operator $(D\Delta^2 - \mu_1\omega^2)$. The solution u of equation (26) is sought in the following form:

$$u(M) = V_1 - \varepsilon\omega^2\mu\gamma_1 * \left\{\alpha u + \int_\Sigma u\mathscr{G}_\omega\right\}(M) + \gamma_1 * [s_1 + s_2](M)$$

with

$$V_1 = \gamma_1 * [F - P_0](M). \tag{27}$$

Then u and the boundary sources s_1 and s_2 are expanded into Taylor series:

$$u = u^0 + \varepsilon u^1 + \varepsilon^2 u^2 + \ldots,$$

$$s_1 = s_1^0 + \varepsilon s_1^1 + \varepsilon^2 s_1^2 + \ldots,$$

$$s_2 = s_2^0 + \varepsilon s_2^1 + \varepsilon^2 s_2^2 + \ldots.$$

The zero order approximation is the solution of the boundary integral equations

$$\ell\gamma_1 * [s_1^0 + s_2^0](M) = \ell V_1(M), \qquad \ell'\gamma_1 * [s_1^0 + s_2^0](M) = \ell' V_1(M), \qquad \forall M \in \partial\Sigma, \tag{28}$$

with

$$u^0(M) - \gamma_1 * [s_1^0 + s_2^0](M) = V_1(M), \qquad \forall M \in \Sigma.$$

Now let $\Gamma[u]$ be the operator defined by

$$\Gamma[u](M) = \int_\Sigma \int_\Sigma \gamma_1(M, M'')\mathscr{G}_\omega(M', M'')u(M')\,d\sigma(M')\,d\sigma(M'').$$

The first order correcting terms are the solutions of the following boundary integral equations:

$$\ell\gamma_1 * [s_1^1 + s_2^1](M) = \omega^2\mu\ell\{\alpha\gamma_1 * u^0(M) + \Gamma[u^0](M)\},$$

$$\ell'\gamma_1 * [s_1^1 + s_2^1](M) = \omega^2\mu\ell'\{\alpha\gamma_1 * u^0(M) + \Gamma[u^0](M)\}, \qquad \forall M \in \partial\Sigma, \tag{29}$$

with

$$u^1(M) - \gamma_1 * [s_1^1 + s_2^1](M) = -\omega^2\mu\{\alpha\gamma_1 * u^0(M) + \Gamma[u^0](M)\}, \qquad \forall M \in \Sigma.$$

These equations are easy to write explicitly for any set of boundary conditions.

2.6. FAR FIELD ACOUSTIC PRESSURE

Let (r, θ, φ) be the co-ordinates of a point Q in a spherical system, the origin of which is on the plane $z = 0$. It is well known that the sound pressure radiated by the plate in the far field is related to the Fourier transform of its displacement by:

$$p^+(Q) - p_0^+(Q) \simeq -\frac{e^{ikr}}{2\pi r}\,\hat{u}(k\sin\theta\cos\varphi, k\sin\theta\sin\varphi) \quad \text{for} \quad 0 < \theta < \pi/2,$$

$$p^-(Q) - p_0^-(Q) \simeq +\frac{e^{ikr}}{2\pi r}\,\hat{u}(k\sin\theta\cos\varphi, k\sin\theta\sin\varphi) \quad \text{for} \quad \pi/2 < \theta < \pi,$$

$$\hat{u}(\xi, \eta) = \int_\Sigma u(x, y)\, e^{-i(x\xi + y\eta)}\, dx\, dy.$$

If the modal series representation of the plate displacement is used, the far field acoustic pressure involves the Fourier transform of the *in vacuo* modes which are used in the approximations. For a rectangular plate, these modes are combinations of exponential functions, the Fourier transforms of which are known analytically. For more complex geometries, a Fast Fourier Transform algorithm is very convenient.

The boundary integral representation of the plate displacement requires more numerical computation. The plate displacement has the following form:

$$u \simeq \gamma_1 * \{F - P_0 + s_1^0 + s_2^0\} - \varepsilon\omega^2\mu\gamma_1 * \left\{\alpha u^0 - \int_\sigma \mathscr{G}_\omega u^0 + s_1^1 + s_2^1\right\},$$

with

$$u^0 = \gamma_1 * \{F - P_0 + s_1^0 + s_2^0\}.$$

The Fourier transform of the convolution products is, of course, the product of the Fourier transforms of each term. For a two-dimensional plate, the transform of the kernel γ_1 is

$$\hat{\gamma}_1(\xi, \eta) = D^{-1}[(\xi^2 + \eta^2)^2 - \mu_1\omega^2]^{-1}.$$

In simple cases, the Fourier transform of F or P_0 can be obtained analytically, but, in general, it requires a numerical integration. The Fourier transforms of the boundary sources involve integrals along the plate boundary which are, in general, evaluated numerically. Finally, in our opinion, the Fourier transform of the last term $\int_\sigma \mathscr{G}_\omega u^0$ can be calculated numerically only.

2.7. A SIMPLE EXAMPLE

The method which has been developed in this section is now illustrated by a simple two-dimensional example. The plate is a beam of constant width $2L$ and infinite length. It is excited by a line force of constant strength along its symmetry axis and there is no acoustic source. So the plate equation reduces to a one-dimensional equation, and the radiated pressure is governed by a two-dimensional homogeneous Helmholtz equation.

The calculations have been conducted for the following numerical data: plate width $2L = 2$ m; plate thickness $h = 0{\cdot}01$ m; mass of the plate per unit area $\mu = 78$ kg/m^2; Young's modulus $E = 2{\cdot}26\ 10^{11}$ Pa: Poisson's ratio $v = 0{\cdot}28$; stiffness $D = 2{\cdot}04 \times 10^4$ Nm; fluid density $\mu_0 = 1{\cdot}29$ kg/m^3; sound speed $c_0 = 340$ m/s; this gives $\mu/\mu_0 = 1{\cdot}65 \times 10^{-2}$ m^{-1}. The coincidence frequency is 1137 Hz; this gives $\tilde{L}_c = 0{\cdot}299$ m and $\tilde{\mu}/\tilde{\mu}_0 = 4{\cdot}95 \times 10^{-3}\ \lambda_c^{-1}$.

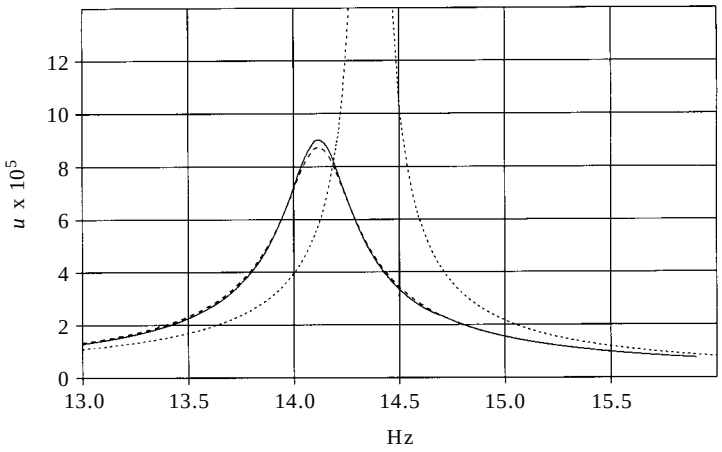

Figure 1. Displacement of the plate around the first *in vacuo* resonance mode. ——, Exact solution; – – – –, approximation; · · · · ·, *in vacuo* displacement.

The first set of results, from reference [1], concerns the approximation of the modal representation of the solution. It is well known that the air-loaded plate response is rather similar to the *in vacuo* one as far as the excitation frequency, which is not too close to the resonance frequency of the plate, is concerned. So, to prove the efficiency of the perturbation method, the plate response has been calculated around its first, third and fifth resonance frequencies. In Figures 1–3, the approximate solution is compared to the numerical solution of the exact boundary integral equations.

A second set of curves concerns the application of the perturbation for solving the boundary integral equations which govern the fluid/plate interactions. Some of them are from reference [10]. The plate displacement is calculated for different frequencies. The zero and first order approximations are compared to the numerical solution of the exact equations. In a first set of curves (Figures 4–6), a value α_1 of the damping coefficient α has been estimated by using the plate displacement of an infinite *in vacuo* plate. For the second set (Figures 7–9), a second value α_2 has been calculated by taking the plate displacement of a finite length plate with a damping factor equal to α_1: this second estimation is more accurate because it involves a displacement which satisfies the boundary conditions.

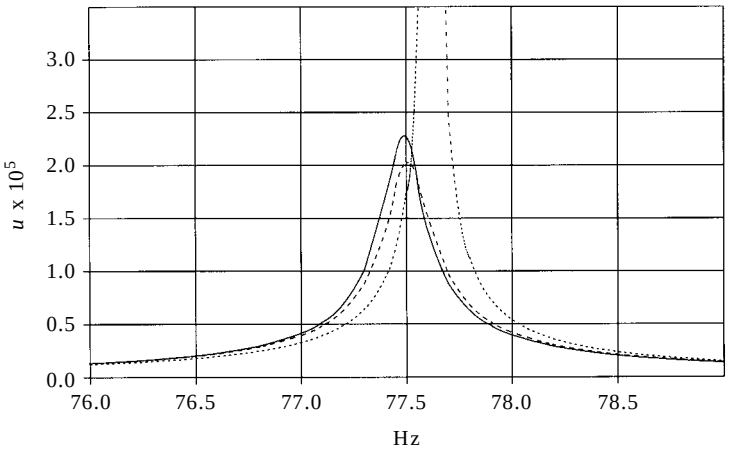

Figure 2. As Figure 1 but around the third *in vacuo* resonance mode.

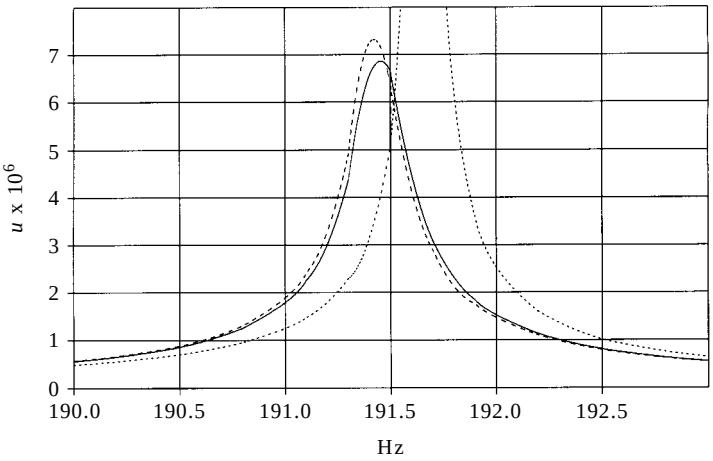

Figure 3. As Figure 1 but around the fifth *in vacuo* resonance mode.

The first three curves show that the perturbation method is a much more powerful method to compute the series representation of the solution in terms of the fluid-loaded plate resonance modes. The results suggest that the fluid-loaded plate equation can be replaced by an *in vacuo* plate equation for a damped material with a slightly higher density: the damping factor and the excess mass, which *a priori* both depend on the frequency, are given by the complex resonance frequencies which are accurately evaluated by a perturbation method. This result is, of course, not new.

The curves of Figures 4–6 show that the first order approximation obtained with a rough estimate of the damping factor α is not very good, though it is not so bad. With a much better estimate of this damping factor, the approximations are very good, even the zero order ones, as shown by Figures 7–9.

Finally, it must be noted that the numerical results presented here have been obtained for frequency domains in the close vicinity of an *in vacuo* plate resonance frequency, which

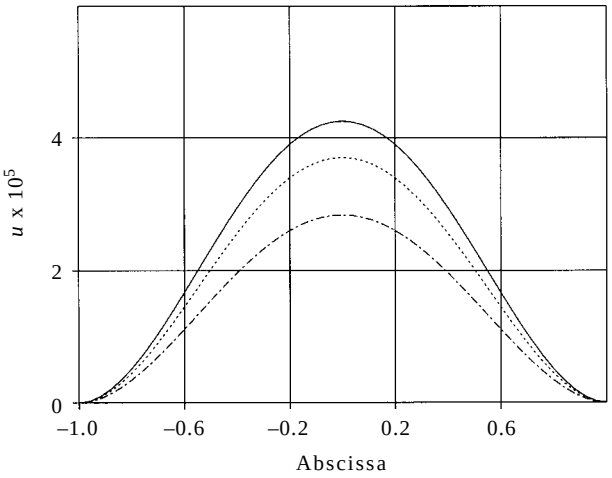

Figure 4. Displacement of the plate at the first *in vacuo* resonance mode: comparison between the numerical solution of the exact equations and zero and first order approximations for $\alpha = \alpha_1$. ——, Exact; –·–·–, order 0; ----, order 1.

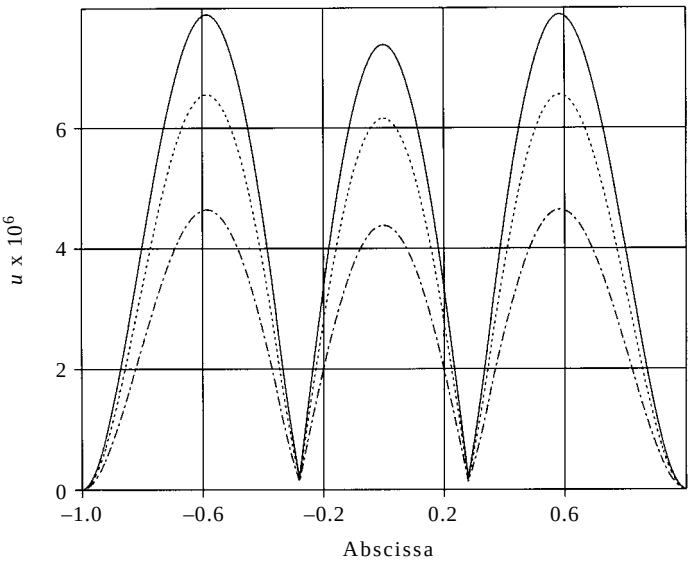

Figure 5. As Figure 4 but at the third *in vacuo* resonance frequency.

is one of the most disadvantageous situations. In real life, acousticians are more interested in global noise levels within rather large frequency bandwidths (octave or third of an octave) which are less sensitive to errors concentrated around discrete frequencies.

3. RESPONSE OF A STRUCTURE TO THE WALL PRESSURE OF A TURBULENT FLOW: RESONANCE MODES SERIES AND LIGHT FLUID APPROXIMATION

The aim in this section is twofold. First, we are interested in the vibro-acoustic response of a simple structure (a baffled plate closing a cavity and immersed in a fluid) to the wall

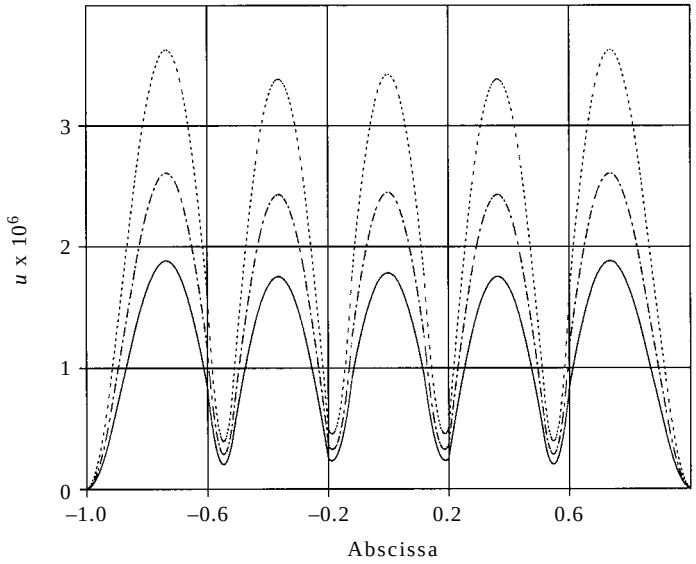

Figure 6. As Figure 4 but at the fifth *in vacuo* resonance frequency.

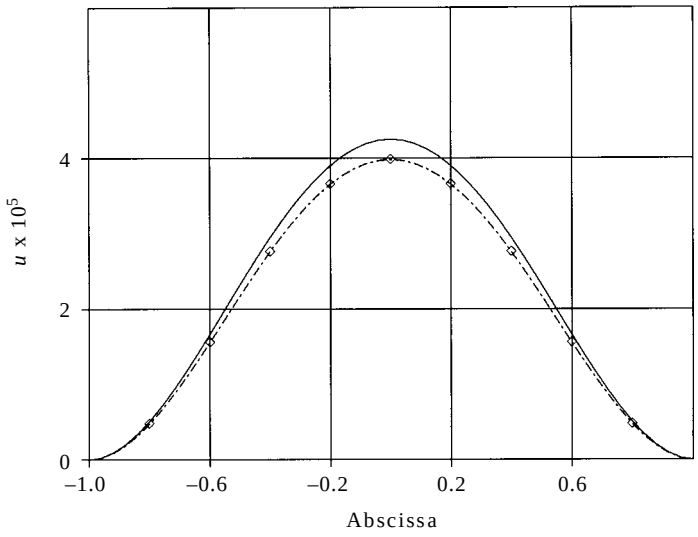

Figure 7. As Figure 4 but for $\alpha = \alpha_2$. ——, Exact; –·–·–, order 0; —◇—, order 1.

pressure that is exerted by a random process—and, more specially, a turbulent boundary layer—which depends randomly on both the time and the space variables. The statistical properties of the plate displacement and of the radiated pressure are easily related to those of the excitation process as a series of the resonance modes of the system structure/fluid. Second, when the fluid is a gas, a perturbation method enables one to express the fluid-loaded resonance modes of the system from the *in vacuo* plate resonance modes on the one hand, and from the rigidly closed cavity modes on the other. The theoretical aspect developed here was partly presented in reference [11].

Consider the same baffled plate as in the preceding section. The domain Ω^+ is the half-space $z > 0$. The domain Ω^- is contained in the half-space $z < 0$ and bounded by Σ

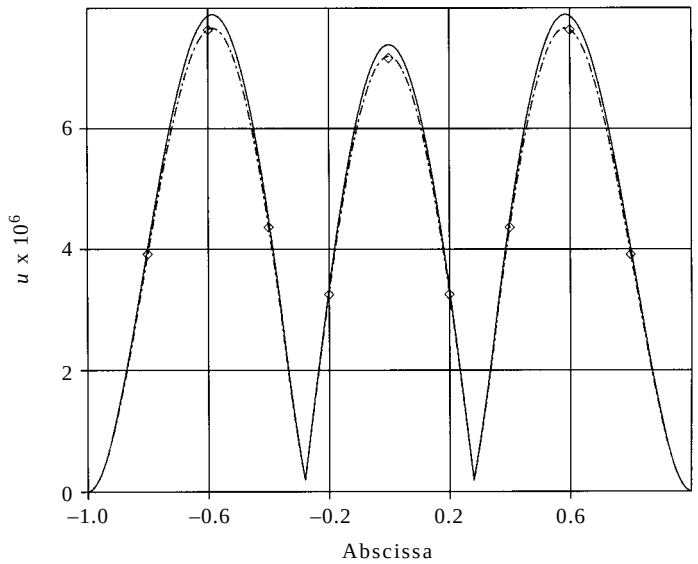

Figure 8. As Figure 5 but for $\alpha = \alpha_2$. ——, Exact; –·–·–, order 0; —◇—, order 1.

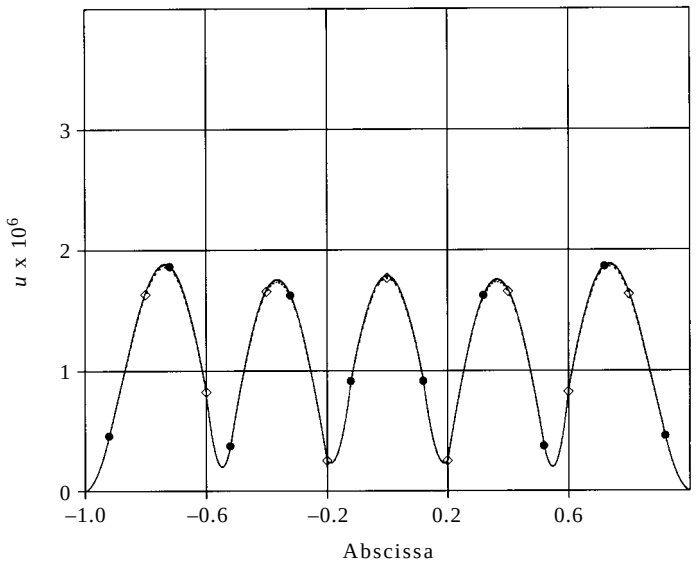

Figure 9. As Figure 6 but for $\alpha = \alpha_2$. ——, Exact; –●–, order 0; —◇—, order 1.

and a surface σ with exterior normal unit vector $\hat{\mathbf{v}}$. The domains Ω^- and Ω^+ are filled with a gas. The mechanical characteristics of the system are the same as in the preceding section.

The only energy source is a wall pressure exerting on the plate, with a density described by the process $f(M; t)$ which depends randomly on M and t. This process is assumed to be stationary up to order two with respect to the time variable and, thus, can be characterized by a cross-spectrum power density $S_f(M, M'; \omega)$, where M and M' are two points in the plane $z = 0$ and ω is the angular frequency.

Let $\tilde{u}(M; t)$ denote the plate displacement, $\tilde{p}^+(Q; t)$ the acoustic pressure radiated into Ω^+ and $\tilde{p}^-(Q; t)$ the acoustic pressure in the cavity Ω^-. Each realization of these processes satisfies the following boundary value problem:

$$\left(\Delta - \frac{1}{c_0^2}\frac{\partial^2}{\partial t^2}\right)\tilde{p}^{\pm}(Q; t) = 0, \qquad Q \in \Omega^{\pm},$$

$$\left(D\Delta^2 + \mu\frac{\partial^2}{\partial t^2}\right)\tilde{u}(M; t) = f(M; t) - \mathrm{Tr}\tilde{p}^+(M; t) + \mathrm{Tr}\tilde{p}^-(M; t), \qquad M \in \Sigma,$$

$$\begin{aligned}
\mathrm{Tr}\,\partial_z\tilde{p}^{\pm}(M; t) &= -\mu_0\,\partial^2\tilde{u}(M, t)/\partial t^2, && M \in \Sigma,\\
\mathrm{Tr}\,\partial_z\tilde{p}^{+}(M; t) &= 0, && M \in \Sigma',\\
\mathrm{Tr}\,\partial_{\mathbf{v}}\tilde{p}^{-}(M; t) &= 0, && M \in \sigma',\\
\ell\tilde{u}(M; t) = \ell'\tilde{u}(M; t) &= 0, && M \in \partial\Sigma.
\end{aligned} \tag{30}$$

A Neumann boundary condition has been arbitrarily adopted on σ, but any other condition can be used.

The response of the system is given by the fields of cross-spectrum densities between the different quantities: the plate displacement and the exterior and interior acoustic pressures. Attention will be paid to three of them only—$S_u(M, M'; \omega)$, $S_{p^+}(Q, Q'; \omega)$ and $S_{p^-}(Q, Q'; \omega)$—which seems to be of main interest. Nevertheless, other cross-spectrum densities can easily be obtained in the same way.

First consider the response of the system to a point harmonic unti force $\delta_{M'}\,\mathrm{e}^{-\mathrm{i}\omega t}$. The corresponding plate displacement and pressure fields are respectively denoted by $u_{M'}(M;\omega)$, $p^{+}_{M'}(Q;\omega)$ and $p^{-}_{M'}(Q;\omega)$. They obey the following equations:

$$
\begin{gathered}
(\Delta + \omega^2/c_0^2)p^{\pm}_{M'}(Q;\omega) = 0, \qquad Q\in\Omega^{\pm},\\
(D\Delta^2 - \mu\omega^2)u_{M'}(M;\omega) = \delta_{M'} - \operatorname{Tr} p^{+}_{M'}(M;\omega) + \operatorname{Tr} p^{-}_{M'}(M;\omega), \qquad M\in\Sigma,\\
\operatorname{Tr}\partial_z p^{\pm}_{M'}(M;\omega) = \mu_0\omega^2 u_{M'}(M;\omega), \qquad M\in\Sigma,\\
\operatorname{Tr}\partial_z p^{+}_{M'}(M;\omega) = 0, \qquad M\in\Sigma',\\
\operatorname{Tr}\partial_{\mathbf{v}} p^{-}_{M'}(M;\omega) = 0, \qquad M\in\sigma,\\
\ell u_{M'}(M;\omega) = \ell' u_{M'}(M;\omega) = 0, \qquad M\in\partial\Sigma.
\end{gathered}
\tag{31}
$$

The uniqueness of the solution is ensured by a convenient Sommerfeld condition on $p^{+}_{M'}(Q;\omega)$ (or any equivalent condition). Let $\mathscr{G}_{\omega}(Q,Q')$ be the Green function for the Neumann problem in Ω^{+}. Then, the exterior acoustic pressure can be expressed as an integral of the plate displacement:

$$
p^{+}_{M'}(Q;\omega) = \mu_0\omega^2\int_{\Sigma} u_{M'}(M;\omega)\mathscr{G}_{\omega}(Q,M)\,\mathrm{d}\Sigma(M).
$$

By introducing this expression into the first of equations (31), one is left with two unknown functions $u_{M'}(M;\omega)$ and $p^{-}_{M'}(Q;\omega)$ only.

Using a classical proof [12], the following results can be established:

$$
\begin{aligned}
S_u(M,M';\omega) &= \int_{\Sigma}\int_{\Sigma} u_N(M;\omega)S_f(N,N';\omega)u^{*}_{N'}(M';\omega)\,\mathrm{d}\Sigma(N)\,\mathrm{d}\Sigma(\mathrm{N}'),\\
S_{p^{+}}(Q,Q';\omega) &= \int_{\Sigma}\int_{\Sigma} p^{+}_{N}(Q;\omega)S_f(N,N';\omega)p^{+}_{N'}{}^{*}(Q';\omega)\,\mathrm{d}\Sigma(N)\,\mathrm{d}\Sigma(\mathrm{N}'),\\
S_{p^{-}}(Q,Q';\omega) &= \int_{\Sigma}\int_{\Sigma} p^{-}_{N}(Q;\omega)S_f(N,N';\omega)p^{-}_{N'}{}^{*}(Q';\omega)\,\mathrm{d}\Sigma(N)\,\mathrm{d}\Sigma(\mathrm{N}').
\end{aligned}
\tag{32}
$$

The mostly used models of turbulence, like those of references [13] and [14], express the cross-spectrum power density of the wall pressure as an inverse space Fourier transform,

$$
S_f(M,M';\omega) = \int_{R^2} S(\Xi;\omega)\,\mathrm{e}^{2\mathrm{i}\pi(\mathbf{M}-\mathbf{M}')\cdot\boldsymbol{\Xi}}\,\mathrm{d}\xi_1\,\mathrm{d}\xi_2,
$$

where $\mathbf{M}$ (resp. $\mathbf{M}'$) is the vector with components the co-ordinates of M (resp. M'), and $\boldsymbol{\Xi}$ is the vector with components (ξ_1,ξ_2), dual of (x,y) in the space Fourier transform. Let $U(M,\Xi;\omega)$ be the plate displacement due to the force $\mathrm{e}^{2\mathrm{i}\pi\mathbf{M}\cdot\boldsymbol{\Xi}}$ (Ξ being the point with co-ordinates ξ_1 and ξ_2). Then the various cross-spectrum power densities of the system response can be expressed in terms of this displacement; one has, for example,

$$
S_u(M,M';\omega) = \int_{R^2} U(M,\Xi;\omega)S(\Xi;\omega)U^{*}(M,\Xi;\omega)\,\mathrm{d}\xi_1\,\mathrm{d}\xi_2.
$$

In the next section, the cross-spectrum power densities are expanded into a series of the resonance modes of the system cavity/plate/external fluid. Then a second section is devoted to the light fluid approximation of the resonance modes. A third section presents a numerical example which illustrates the behaviour of the system.

3.1. EIGENMODES AND RESONANCE MODES: RESONANCE MODES SERIES REPRESENTATION OF THE SOLUTION

One introduces the following bi-linear forms:

$$\langle u, v\rangle = \int_\Sigma u(M)v^*(M)\,\mathrm{d}\sigma(M), \qquad \langle\!\langle p, \psi\rangle\!\rangle = \int_{\Omega^-} p\psi^*\,\mathrm{d}\Omega,$$

$$a(u, v) = D\int_\Sigma \left\{\Delta u\Delta v^* + (1-\nu)\left[2\frac{\partial^2 u}{\partial x\,\partial y}\frac{\partial^2 v^*}{\partial x\,\partial y} - \frac{\partial^2 u}{\partial x^2}\frac{\partial^2 v^*}{\partial y^2} - \frac{\partial^2 u}{\partial y^2}\frac{\partial^2 v^*}{\partial x^2}\right]\right\}\mathrm{d}\sigma(M),$$

$$\beta_\omega(u, v) = \int_\Sigma\int_\Sigma u(M)\mathscr{G}_\omega(M, M')v^*(M')\,\mathrm{d}\sigma(M)\,\mathrm{d}\sigma(M'). \tag{33}$$

The weak form of system (31) is

$$\begin{aligned} &a(u_{M'}, v) - \langle \mathrm{Tr}\, p^-_{M'}, v\rangle - \mu\omega^2\{\langle u_{M'}, v\rangle - \eta^2\beta_\omega(u_{M'}, v)\} = v^*(M'),\\ &-\langle\!\langle \nabla p^-_{M'}, \nabla\psi\rangle\!\rangle + \frac{\omega^2}{c_0^2}\langle\!\langle p^-_{M'}, \psi\rangle\!\rangle + \mu_0\omega^2\langle u_{M'}, \mathrm{Tr}\psi\rangle = 0, \end{aligned} \tag{34}$$

with $\eta^2 = \mu_0/\mu$. In these equations, v and ψ are, as usual, test functions which belong to convenient functional spaces.

3.1.1. *Eigenmodes and resonance modes*

The eigenmodes (U_n, P_n) of the coupled system fluid-loaded plate/cavity and the eigenvalues Λ_n are defined by

$$\begin{aligned} &a(U_n, v) - \langle \mathrm{Tr}\, P_n, v\rangle = \mu\Lambda_n\{\langle U_n, v\rangle - \eta^2\beta_\omega(U_n, v)\},\\ &-\langle\!\langle \nabla P_n, \nabla\psi\rangle\!\rangle + \mu_0\omega^2\langle U_n, \mathrm{Tr}\psi\rangle = -(\Lambda_n/c_0^2)\langle\!\langle P_n, \psi\rangle\!\rangle. \end{aligned} \tag{35}$$

This definition corresponds to that given in reference [7] (section 9.4). By using a similar method as that of reference [1], an orthogonality relationship can be established:

$$\begin{aligned} &\langle\!\langle P_n, P_q^*\rangle\!\rangle/\omega^2\mu_0 c_0^2 + \mu[\langle U_n, U_q^*\rangle - \eta^2\beta_\omega(U_n, U_q^*)] = 0 \quad \text{if} \quad n \neq q,\\ &\langle\!\langle P_q, P_q^*\rangle\!\rangle/\omega^2\mu_0 c_0^2 + \mu[\langle U_q, U_q^*\rangle - \eta^2\beta_\omega(U_q, U_q^*)] = N_q \quad \text{if} \quad n = q. \end{aligned} \tag{36}$$

Obviously, U_n, P_n and Λ_n are frequency dependent.

The resonance modes (w_n, Ψ_n) and the corresponding resonance angular frequencies ω_n are the non-trivial solutions of the following variational problem:

$$\begin{aligned} &a(w_n, v) - \langle \mathrm{Tr}\, \Psi_n, v\rangle = \mu\omega_n^2\{\langle w_n, v\rangle - \eta^2\beta_\omega(w_n, v)\},\\ &-\langle\!\langle \nabla\Psi_n, \nabla\psi\rangle\!\rangle + \mu_0\omega_n^2\langle w_n, \mathrm{Tr}\psi\rangle = -(w_n^2/c_0^2)\langle\!\langle \Psi_n, \psi\rangle\!\rangle. \end{aligned} \tag{37}$$

It does not seem possible to establish an orthogonality relationship between the resonance modes (at least, the authors have not been able to do so).

3.1.2. *Series representation of the response of the system to a harmonic or transient deterministic excitation*

In what follows, it is assumed that there exists a sequence of eigenmodes which is a basis in terms of which solution can be expanded. As has been done in section 2, the solution $(u_{M'}, p^-_{M'})$ of equation (31) is expanded into series of the eigenmodes, leading to the result

$$u_{M'}(M;\omega) = \sum_{n=1}^{\infty} \alpha_n(M';\omega) U_n(M), \qquad p^-_{M'}(Q;\omega) = \sum_{n=1}^{\infty} \alpha_n(M';\omega) P_n(Q),$$

with

$$\alpha_n(M') = U_n(M')/(\Lambda_n - \omega^2)N_n.$$

The acoustic pressure radiated into the half-space Ω^+ is given by

$$p^+_{M'}(Q) = \sum_{n=1}^{\infty} \alpha_n(M';\omega) P^+_n(Q),$$

with

$$p^+_n(Q) = \mu_0 \omega^2 \int_\Sigma U_n(M) \mathscr{G}_\omega(Q, M)\, \mathrm{d}\Sigma(M). \tag{39}$$

To obtain a series representation of the solution in terms of the resonance modes, that is

$$u_{M'}(M;\omega) = \sum_n \beta_n(M';\omega) w_n(M), \qquad p^-_{M'}(Q;\omega) = \sum_n \beta_n(M';\omega) \Psi_n(Q),$$

one proceeds as in the first example by looking at the impulse response of the system. It is expressed by an inverse Fourier transform:

$$\tilde{u}_{M'}(M;t) = \sum_{n=1}^{\infty} \frac{1}{2\pi} \int_{-\infty}^{+\infty} \frac{U_n(M')U_n(M)}{N_n(\omega)(\Lambda_n - \omega^2)} \mathrm{e}^{-\mathrm{i}\omega t}\, \mathrm{d}\omega.$$

The integrals are calculated by the residues method which involves the roots of the sequence of equations $D_n(\omega) = \Lambda_n(\omega) - \omega^2$, which are the resonance angular frequencies. It can be shown that two resonance angular frequencies are associated with each $\Lambda_n(\omega)$ and they will be denoted by $\omega_n = \Omega_n - \mathrm{i}\tau_n$ and $\omega_{-n} = -\Omega_n - \mathrm{i}\tau_n$. The resonance frequencies are assumed to have negative imaginary parts ($\tau_n > 0$). It can be shown also that the resonance mode (w_{-n}, Ψ_{-n}) is the complex conjugate of (w_n, Ψ_n).

Let $\Lambda'_n(\omega)$ be the derivative of $\Lambda_n(\omega)$ with respect to ω. Then the displacement of the plate due to an impulse unit point force is zero for negative times and, for $t > 0$, is given by

$$\tilde{u}_{M'}(M;t) = -\mathrm{i} \sum_{n=1}^{\infty} \left[\frac{w_n(M')w_n(M)}{N_n(\omega_n)[\Lambda'_n(\omega_n) - 2\omega_n]} \mathrm{e}^{-\mathrm{i}\Omega_n t} \right.$$

$$\left. - \frac{w^*_n(M')w^*_n(M)}{N^*_n(\omega_n)[\Lambda'^*_n(\omega_n) - 2\omega^*_n]} \mathrm{e}^{+\mathrm{i}\Omega_n t} \right] \mathrm{e}^{-\tau_n t}. \tag{40}$$

The corresponding expressions of the acoustic pressure fields are

$$p_{M'}^{-}(Q;\omega)=\sum_{n=1}^{\infty}\left[\frac{w_n(M')\Psi_n(Q)}{N_n(\omega_n)[\Lambda_n'(\omega_n)-2\omega_n](\omega-\omega_n)}\right.$$

$$\left.-\frac{w_n^*(M')\Psi_n^*(Q)}{N_n^*(\omega_n)[\Lambda_n'^*(\omega_n)-2\omega_n^*](\omega+\omega_n^*)}\right]. \tag{41}$$

$$p_{M'}^{+}(Q;\omega)=\sum_{n=1}^{\infty}\left[\frac{w_n(M')\mu_0\omega_n^2}{N_n(\omega_n)[\Lambda_n'(\omega_n)-2\omega_n](\omega-\omega_n)}\int_{\Sigma}w_n(M)\mathscr{G}_{\omega_n}(M,Q)\,\mathrm{d}\Sigma(M)\right.$$

$$\left.-\frac{w_n^*(M')\mu_0\omega_n^{*2}}{N_n^*(\omega_n)[\Lambda_n'^*(\omega_n)-2\omega_n^*](\omega+\omega_n^*)}\int_{\Sigma}w_n^*(M)\mathscr{G}_{\omega_n}^*(M,Q)\,\mathrm{d}\Sigma(M)\right]. \tag{42}$$

The coefficients which occur in the expansions (40)–(42) are solutions of an infinite system of linear algebraic equations. The most classical method of computing an approximation to these coefficients is to solve a truncated form of the linear system that they satisfy. Another way is to find an approximation of the derivative $\Lambda_n'(\omega)$ of the $\Lambda_n(\omega)$ with respect to ω: it can be obtained numerically, or analytically if the assumption of light coupling can be made.

3.1.3. *Resonance modes series representation of the response of the system to a random process*

The representation is given by introducing the series (40)–(42) into expressions (32). One first defines the following set of constants:

$$A_n=1/N_n[\Lambda_n'-\omega_n],$$

$$\chi_{nm}^1=\int_{\Sigma}\int_{\Sigma}w_n(N)S_f(N,N';\omega)w_m^*(N')\,\mathrm{d}\Sigma(N)\,\mathrm{d}\Sigma(N'),$$

$$\chi_{nm}^2=\int_{\Sigma}\int_{\Sigma}w_n(N)S_f(N,N';\omega)w_m(N')\,\mathrm{d}\Sigma(N)\,\mathrm{d}\Sigma(N'),$$

$$\chi_{nm}^3=\int_{\Sigma}\int_{\Sigma}w_n^*(N)S_f(N,N';\omega)w_m^*(N')\,\mathrm{d}\Sigma(N)\,\mathrm{d}\Sigma(N'). \tag{43}$$

Then the cross power spectrum density of the displacement takes the form

$$S_u(M,M';\omega)=\sum_{n=1}^{\infty}\sum_{m=1}^{\infty}\frac{A_nw_n(M)}{\omega-\omega_n}\chi_{nm}^1\frac{A_m^*w_m^*(M')}{\omega-\omega_m^*}$$

$$+\sum_{n=1}^{\infty}\sum_{m=1}^{\infty}\frac{A_n^*w_n^*(M)}{\omega+\omega_n^*}\chi_{nm}^1\frac{A_mw_m(M')}{\omega+\omega_m}-\sum_{n=1}^{\infty}\sum_{m=1}^{\infty}\frac{A_nw_n(M)}{\omega-\omega_n}\chi_{nm}^2\frac{A_mw_m(M')}{\omega+\omega_m}$$

$$-\sum_{n=1}^{\infty}\sum_{m=1}^{\infty}\frac{A_n^*w_n^*(M)}{\omega+\omega_n^*}\chi_{nm}^3\frac{A_m^*w_m^*(M')}{\omega-\omega_m^*}. \tag{44}$$

Similar expressions can be established for other cross-power-density spectra, in particular those for acoustic pressure fields.

This last representation of the response of the system is very convenient to show how the resonance modes govern the vibro-acoustic behaviour of the system. For an angular frequency ω close to the real part Ω_q of the resonance angular frequency ω_q, the qth term in the first series of expression (44) is much larger than the other ones and is expected to provide a good approximation of $S_u(M, M'; \omega)$. As will be seen later on the numerical curves, the various power density spectra have sharp peaks around the real part of each resonance frequency, and vary very smoothly in between. This suggests that a good approximation to the system response can be obtained by accurately computing its behaviour in the vicinity of these frequencies and using a rough interpolation in between.

3.2. LIGHT FLUID APPROXIMATION

When the fluid is a gas, it has a weak influence on the vibration regime of the elastic structure. This implies that the system cavity/plate/external fluid will have two types of resonance modes: a first category corresponds to resonance angular frequencies close to the *in vacuo* plate resonance frequencies (they are often called *plate* modes); the second one corresponds to frequencies close to those of the rigidly closed cavity modes: that is, modes which satisfy a Neumann condition along the plate surface (they are often called *cavity* modes).

In general, the resonance frequencies and the resonance modes are determined by numerically solving the exact equations; there are very few examples for which an analytical solution is possible. It will be shown now that, for weak coupling between the solid and the fluid, an analytical approximation for the resonance frequencies and the resonance modes can easily be found. The coupled resonance frequencies and resonance modes are expressed in terms of the plate and cavity resonance frequencies and resonance modes. If the plate and cavity resonance frequencies and resonance modes are known analytically, then one obtains a completely analytical approximation for the coupled system; if they are known numerically only, one is left with a mixed numerical/analytical approximation.

3.2.1. *Approximation of the equations governing the resonance modes of the system cavity/plate/external fluid*

As already recalled, the general bases of the perturbation method presented here are classical and described in many text books. Among the various papers dealing with a weak coupling between a structure and a fluid that we have read, references [15] and [16] present results rather close to ours. The authors look for an approximation of the response of a fluid-loaded structure to a harmonic excitation as a series of the *in vacuo* structure modes. Reference [17] must also be mentioned, in which the authors use the response of a membrane to a turbulent flow to measure the parameters involved in a turbulence model: to get an easy method, use is made of a light fluid approximation, the validity conditions of which are carefully presented.

Our approach is quite different from that of the above cited papers. The first step is to define the resonance modes of the complete system and to expand its response into a series of these modes; the second step is to develop a light fluid approximation of the resonance frequencies and the resonance modes. They are sought as formal Taylor series in the small parameter $\eta = (\mu_0/\mu)^{1/2}$:

$$\begin{aligned} w_n &= w_n^0 + \eta w_n^1 + \eta^2 w_n^2 + \dots, \\ \Psi_n &= \Psi_n^0 + \eta \Psi_n^1 + \eta^2 \Psi_n^2 + \dots, \\ \omega_n^2 &= \Lambda_n^0 + \eta \Lambda_n^1 + \eta^2 \Lambda_n^2 + \dots. \end{aligned} \tag{45}$$

It is clear that η^2 has the dimension of the inverse of a length and that one might prefer to use a dimensionless parameter. As already mentioned, in our opinion, it is useless to try to find one.

The weak (energetic) form of the equations governing the resonance modes is

$$a(w_n, v) - \langle \mathrm{Tr}\ \Psi_n, v\rangle - \mu\omega^2\{\langle w_n, v\rangle - \eta^2\beta_\omega(w_n, v)\} = 0$$

$$-\langle\!\langle \nabla\Psi_n, \nabla\psi\rangle\!\rangle + \frac{\omega^2}{c_0^2}\langle\!\langle \Psi_n, \psi\rangle\!\rangle + \mu_0\omega^2\langle w_n, \mathrm{Tr}\ \psi\rangle = 0. \tag{46}$$

Expansions (45) are introduced into these equations and the successive powers of η are made zero. This leads to the following sequence of equations:
zero order equations,

$$a(w_n^0, v) - \langle \mathrm{Tr}\ \Psi_n^0, v\rangle - \mu\Lambda_n^0\langle w_n^0, v\rangle = 0,$$

$$-\langle\!\langle \nabla\Psi_n^0, \nabla\psi\rangle\!\rangle + (\Lambda_n^0/c_0^2)\langle\!\langle \Psi_n^0, \psi\rangle\!\rangle = 0; \tag{47}$$

first order equations,

$$a(w_n^1, v) - \langle \mathrm{Tr}\ \Psi_n^1, v\rangle - \mu[\Lambda_n^0\langle w_n^1, v\rangle + \Lambda_n^1\langle w_n^0, v\rangle] = 0,$$

$$-\langle\!\langle \nabla\Psi_n^1, \nabla\psi\rangle\!\rangle + (\Lambda_n^0/c_0^2)\langle\!\langle \Psi_n^1, \psi\rangle\!\rangle + (\Lambda_n^1/c_0^2)\langle\!\langle \Psi_n^0, \psi\rangle\!\rangle = 0; \tag{48}$$

second order equations,

$$a(w_n^2, v) - \langle \mathrm{Tr}\ \Psi_n^2, v\rangle - \mu[\Lambda_n^0\langle w_n^2, v\rangle + \Lambda_n^1\langle w_n^1, v\rangle] + \Lambda_n^2\langle w_n^0, v\rangle - \Lambda_n^0\beta_{\Lambda_n^0}(w_n^0, v)] = 0,$$

$$-\langle\!\langle \nabla\Psi_n^2, \nabla\psi\rangle\!\rangle + (\Lambda_n^0/c_0^2)\langle\!\langle \Psi_n^2, \psi\rangle\!\rangle + (\Lambda_n^1/c_0^2)\langle\!\langle \Psi_n^1, \psi\rangle\!\rangle$$

$$+ (\Lambda_n^2/c_0^2)\langle\!\langle \Psi_n^0, \psi\rangle\!\rangle + \mu\Lambda_n^0\langle w_n^0, \mathrm{Tr}\ \psi\rangle = 0. \tag{49}$$

The zero order equations show that three cases must be considered: Λ_n^0 is equal to the square of an *in vacuo* resonance angular frequency of the plate; Λ_n^0 is equal to the square of a resonance angular frequency of the rigidly closed cavity; Λ_n^0 is equal to the square of a resonance angular frequency belonging to both spectra of the *in vacuo* plate and of the rigidly closed cavity.

3.2.2. *Perturbation of an* in vacuo *plate resonance*

Assume that $\Lambda_n^0 = \omega_n^{pl2}$, where ω_n^{pl} is a resonance angular frequency of the *in vacuo* plate, which does not coincide with any resonance angular frequency of the rigidly closed cavity. It is obvious that the zero order approximation of the corresponding plate displacement w_n^0 is identical to V_n, the *in vacuo* plate mode. It is easily seen that the system mode $(w_n^{pl}, \Psi_n^{pl}, \Lambda_n^{pl})$ associated with this resonance frequency is approximated by

$$\Lambda_n^{pl} \simeq \omega_n^{pl2} + \eta^2\Lambda_n^2, \qquad w_n^{pl} \simeq V_n + \eta^2\sum_{q\neq n}\alpha_{nq}V_q, \qquad \Psi_n^{pl} \simeq \eta^2\Psi_n^2, \tag{50}$$

with the following definitions:

$$[\Delta + \omega_n^{pl2}/c_0^2]\Psi_n^2 = 0 \text{ in } \Omega^-, \qquad \mathrm{Tr}\ \partial_z\Psi_n^2 - \mu\omega_n^{pl2}V_n = 0 \text{ on } \Sigma,$$

$$\Lambda_n^2 = \frac{\mu\omega_n^{pl2}\beta_{\omega_n^{pl}}(V_n, V_n^*) - \langle \mathrm{Tr}\ \Psi_n^2, V_n^*\rangle}{\mu\langle V_n, V_n^*\rangle}, \qquad \alpha_{nq} = \frac{\mu\omega_n^{pl2}\beta_{\omega_n^{pl}}(V_n, V_n^*) - \langle \mathrm{Tr}\ \Psi_n^2, V_n^*\rangle}{\mu(\omega_n^{pl2} - \omega_q^{pl2})\langle V_q, V_q^*\rangle}.$$

The coefficient α_{qq} being a solution of an equation of the form $0\,\alpha_{qq} = 0$, it has been chosen arbitrarily to equal zero: such a choice is quite possible because a resonance mode is determined up to an arbitrary normalizing constant. Finally, it must be remarked that the first order terms are identically equal to zero.

3.2.3. *Perturbation of a resonance of the rigidly closed cavity*

One assumes that $\Lambda_n^0 = \omega_n^{c2}$, where ω_n^c is a resonance angular frequency of the rigidly closed cavity (the corresponding mode satisfies a homogeneous Neumann condition on Σ), which is different from any resonance frequency of the *in vacuo* plate. Obviously Ψ_n^0 is identical to the cavity resonance Φ_n. The corresponding resonance mode of the system $(w_n^c, \Psi_n^c, \Lambda_n^c)$ is approximated by

$$\Lambda_n^c = \omega_n^{c2} + \eta^2 \Lambda_n^2, \qquad w_n^c = w_n^0 + \eta^2 w_n^2, \qquad \Psi_n^c = \Phi_n + \sum_{q \neq n} \alpha_{nq} \Phi_q. \tag{51}$$

In these expressions, the different parameters and functions are defined by

$$[\Delta^2 - \mu\omega_n^{c2}] w_n^0 = \mathrm{Tr}\ \Phi_n \text{ in } \Sigma,$$

$$\Lambda_n^2 = -\mu\omega_n^{c2} \frac{\langle w_n^0, \mathrm{Tr}\ \Phi_n^* \rangle}{\langle\langle \Phi_n, \Phi_n^* \rangle\rangle}, \qquad \alpha_{nq} = c_0^2 \omega_n^{c2} \frac{\langle w_n^0, \mathrm{Tr}\ \Phi_q^* \rangle}{(\omega_q^{c2} - \omega_n^{c2}) \langle\langle \Phi_q, \Phi_q^* \rangle\rangle},$$

$$[\Delta^2 - \mu\omega_n^{c2}] w_n^2 = \mathrm{Tr}\ \Phi_n^2 + \mu \left[\Lambda_n^2 w_n^0 - \omega_n^{c2} \int_\Sigma w_n^0 \mathscr{G}_{\omega_n^c} \right] + \sum_{q \neq n} \alpha_{nq}\ \mathrm{Tr}\ \Phi_q \text{ on } \Sigma.$$

In this situation, the first order terms are again identically equal to zero. The correcting term Λ_n^2 is real; the damping effect due to energy radiation into the domain Ω^+ appears in the next non-zero correcting term, the expression for which is easy to establish.

3.2.4. *Perturbation of a plate/cavity resonance*

The last possibility is that the *in vacuo* plate and the rigidly closed cavity have a common resonance angular frequency ω_N^{plc}. Let V_n be the corresponding plate mode, and Φ_q the corresponding cavity mode. The following results can be shown: two resonance frequencies of the coupled system are associated with the common resonance frequency ω_N^{plc}; the first order correcting terms are not zero. The following expressions can be established:

$$\Lambda_N \simeq \omega_N^{plc^2} \pm \eta \Lambda_N^1, \qquad w_N^\pm \simeq V_n + \eta \sum_{s \neq n} \alpha_{ns}^\pm V_s, \qquad \Psi_N^\pm \simeq A^\pm \Phi_q, \tag{52}$$

with

$$\Lambda_N^1 = \omega_N^{plc} c_0 \frac{\langle V_n, \mathrm{Tr}\ \Phi^*{}_q \rangle}{\langle V_n, V_n^* \rangle^{1/2} \langle\langle \Phi_q, \Phi_q^* \rangle\rangle^{1/2}},$$

$$A^\pm = [\omega_N^{plc^2} \pm \eta \Lambda_N^1] \mu \frac{\langle V_n, V_n^* \rangle}{\langle V_n, \mathrm{Tr}\ \Phi_q^* \rangle}, \qquad \alpha_{ns}^\pm = \frac{A^\pm \langle \mathrm{Tr}\ \Phi_q, V_s^* \rangle \pm \mu \Lambda_N^1 \langle V_n, V_s^* \rangle}{\mu[\omega_s^{pl^2} - \omega_N^{plc^2}] \langle V_n, V_n^* \rangle}.$$

Due to the correcting term Λ_n^1 which is real, the common resonance frequency is split into two resonance frequencies of the coupled system which are symmetrical with respect to $\omega_N^{plc^2}$. The damping effect due to energy radiation at infinity in the $z > 0$ half-space appears in the second order correction.

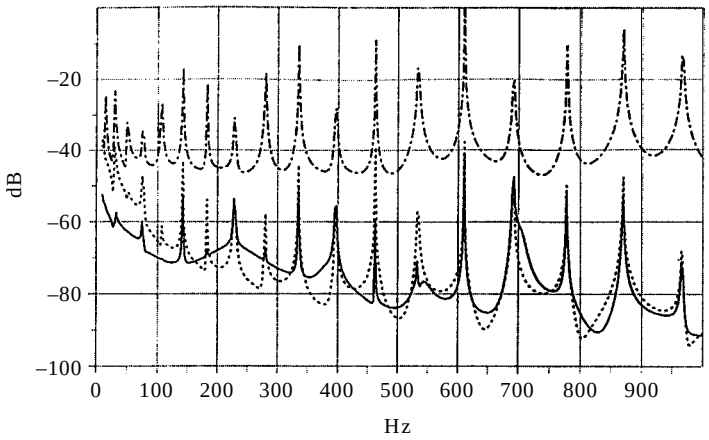

Figure 10. Power density spectra of the response of the system cavity/baffled plate/external fluid to a turbulent wall pressure described by the Corcos model. –.–.–., Acceleration at $x = 0{\cdot}25$ m; ——, pressure in the cavity at $x = 0{\cdot}1$ m, $y = 0{\cdot}4$ m; -----, pressure out of the cavity at $x = 0{\cdot}1$ m, $y = 0{\cdot}4$ m.

3.3. NUMERICAL EXAMPLE

In this section the response of a two-dimensional system cavity/baffled plate/external fluid to a turbulent wall pressure is presented. The plate length is 1 m and its thickness 0·001 m. The cavity dimensions are $1 \times 0{\cdot}77$ m^2 (the interest in such a ratio is that the double resonance modes appear at very high frequencies only). The Young's modulus of the plate material is $2{\cdot}27 \times 10^{11}$ Pa, its Poisson's ratio is 0·28 and its mass per unit area is 7·8 kg/m^2 (steel characteristics). The sound speed in the fluid is 340 m/s and its density is 1·29 kg/m^3 (air characteristics). The plate is excited by the wall pressure due to a turbulent flow which is described by the Corcos model [13]; the flow velocity is 10 m/s.

Our aim being to point out the role played by the resonance modes of the system, a boundary element method is used to solve the exact equations. In Figure 10, it appears that the power density spectra of the plate acceleration and of the external pressure have the same set of sharp peaks which correspond to structure resonances; the power spectrum of the internal acoustic pressure has this set of sharp peaks and, in addition, some soft maxima which correspond to cavity resonances. In Figure 11, the acceleration spectrum

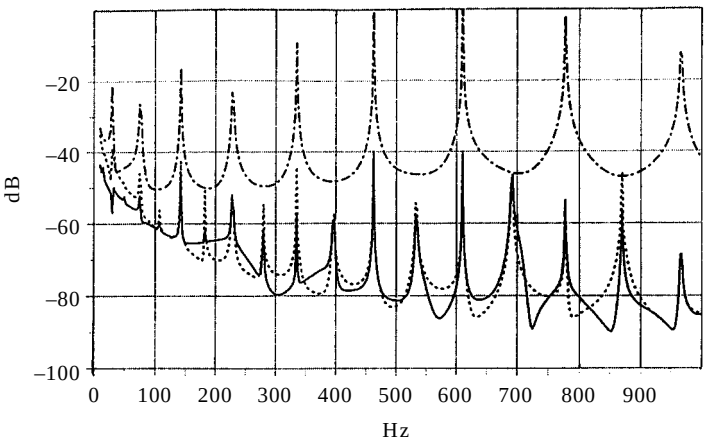

Figure 11. As Figure 10 but –·–·–, acceleration at $x = 0$ m; ——, pressure in the cavity at $x = 0{\cdot}1$ m, $y = 0{\cdot}1$ m; - - - -, pressure out of cavity $x = 0{\cdot}1$ m, $y = 0{\cdot}1$ m.

has one peak every two pressure peaks, only: the missing resonances are odd modes which have a node at the observation point. The pressure spectra are quite similar to the former ones.

These results show what the theoretical analysis has proved: the system response is governed by its resonance modes. These modes can be classified into two categories: structure-born modes which are close to the *in vacuo* structure modes, and cavity modes which are close to the rigidly closed cavity modes. As a consequence, in this case, a perturbation method will be efficient.

Some papers, which deal with similar problems must be mentioned. One of the oldest significant contributions is due to Davies [18]: the author expanded the displacement of a fluid-loaded baffled plate in terms of its *in vacuo* modes and gave an approximation of the series coefficients. A similar approach is followed in references [19, 20]. In two other papers published in 1988 [21, 22], use was made of the fluid-loaded plate Green function to describe its response to a turbulent wall pressure and, then, approximations were given. This last approach is more similar to ours, but the author does not give formulas as explicit as those presented here.

Finally, two recent papers must be mentioned [23, 24]. They deal with the sound induced through an infinite plate excited by the noise generated by a turbulent flow. This is a phenomenon which is slightly different from that studied in this section. Indeed, the plate excitation is not the turbulent wall pressure but the acoustic pressure generated by the vortices, which are moving acoustic sources. In addition, the wave equation written within the moving fluid accounts for this motion. Thus, a resonance peak occurs when the convection velocity is close to the phase speed of the *in vacuo* flexural waves in the plate. Such a phenomenon cannot be described by the equations which are adopted here.

4. EFFICIENCY OF AN ELASTIC SCREEN IN A ROOM

In this section, a perturbation method is applied to a problem of room acoustics. Diffracting thin structures are commonly used in rooms: as reflectors to tune the acoustic performances of a concert hall, and as screens in factory halls to protect workers from machine noise. Most of the computing programmes devoted to room acoustics model these structures as perfectly rigid systems. In practice, they are acoustically excited and, as a consequence, their actual efficiency can differ significantly from the predicted one (this is common for concert halls equipped with a tunable ceiling made of disjoint light panels).

The first aim of this study is to quantify the influence of the vibrations of a screen on its efficiency compared to the efficiency of a perfectly rigid screen. A second aim is to propose a simple numerical method. In the first section the problem is reduced to a boundary integral equation along the screen surface for the two cases, rigid screen and elastic structure. Then a perturbation method is proposed to establish an approximate solution. Finally, the perturbation approximation is compared to the numerical solution of the exact equation. Two examples of dimension two are looked at: a simplified concert hall model in which the structure is parallel to the ceiling and acts as a reflector, and a simplified model of a factory hall in which the structure is orthogonal to the floor and acts as a protecting screen.

The mechanical properties of the structure are varied over a rather wide range. Three situations are pointed out, depending on the rigidity and on the density of the screen material: the vibrations can be neglected; their influence can be predicted by a perturbation method; or the exact equations must be solved.

4.1. BOUNDARY INTEGRAL EQUATION FOR THE SCREEN EFFECT

The room is modelled by a rectangular domain Ω in which a thin screen occupies a segment Σ. The system is excited by a point harmonic ($e^{-i\omega t}$) source located at S. The fluid is characterized by a sound speed c and a density ρ_f.

For simplicity, the boundary $\partial\Omega$ of Ω is characterized by four reflection coefficients (one for each side of the rectangular domain) and the corresponding Green function is approximated by an image method. This simplification has been adopted because most of the computer programmes for room acoustics are based on an image method or a ray method (which is equivalent to the image method when polyhedral boundaries are considered).

4.1.1. *Perfectly rigid screen*

The acoustic pressure field $p(M)$ is the solution of the following boundary value problem:

$$(\Delta + k^2)p(M) = \delta_S(M) \text{ in } \Omega, \qquad \frac{\partial p}{\partial \mathbf{n}}(M) = 0 \text{ on } \Sigma. \tag{53a}$$

Here k is the wavenumber ω/c and $\mathbf{n}$ is the unit vector normal to Σ. Each line segment B_j composing the boundary of the domain Ω is characterized by a reflection coefficient:

$$\beta_j(\, j = 1, \ldots, 4) = \text{reflection coefficient of } B_j, \qquad \text{with } \bigcup_{j=1}^{4} B_j = \partial\Omega. \tag{53b}$$

Let $G(S, M)$ be the Green function of the Helmholtz equation in Ω satisfying the boundary conditions on $\partial\Omega$ defined by the reflection coefficients β_j. It has the form

$$G(S, M) = -\frac{i}{4} H_0^{(1)}(kr(S, M)) - \frac{i}{4} \sum_{n \geqslant 0} A_n H_0^{(1)}(kr(S_n, M)),$$

where S_n, $n = 1, \ldots$ is the nth image of the point source S and A_n is its amplitude which depends on the reflection coefficients; $H_0^{(1)}(z)$ is the Hankel function of the first kind of order 0; and $r(M, M')$ is the distance between the points M and M'.

Let $p_{in}(M)$ be the sound pressure field in the absence of the screen. Then the total pressure can be expressed as [25, 26]

$$p(M) = p_{in}(M) + \int_{\Sigma} \mu(P) \frac{\partial G(M, P)}{\partial \mathbf{n}(P)} \, d\sigma(P). \tag{54}$$

The unknown function μ represents the step of the pressure across the screen.

The boundary value problem is thus replaced by a boundary integral equation:

$$\frac{\partial p_{in}}{\partial \mathbf{n}}(P) - \lim_{P'' \to P} \frac{\partial}{\partial \mathbf{n}(P'')} \int_{\Sigma} \mu(P') \frac{\partial G(P', P'')}{\partial \mathbf{n}(P')} \, d\sigma(P') = 0 \quad \text{on} \quad \Sigma. \tag{55}$$

Here P'' is a point outside Σ with limit P on the screen. It must be recalled that the limit of the normal derivative of a double layer potential is a finite part of the integral: any numerical approximation must be defined carefully (see references [25] and [27], for example). The Green function is computed by using the method described in reference [28].

This integral equation has been solved by a classical collocation method. Σ is divided into N sub-domains Σ_i; to ensure a good accuracy of the numerical solution, the length of each subdomain does not exceed one-sixth of the wavelength in the fluid. The function

μ is approximated by a piecewise constant function, its value on Σ_i being denoted by μ_i, $i = 1, \ldots, N$. The approximate form of equation (55) is then written at N collocation points $P_i \in \Sigma_i$. One is left with a system of N linear algebraic equations to determine the N unknown constants μ_i. The sound pressure field is approximated by introducing the approximation of the layer density μ into the representation (54).

4.1.2. *Elastic screen*

The screen is now modelled as a thin elastic plate. A new unknown function is involved, the transverse displacement u. The sound pressure field p and the plate displacement u are the solutions of a system of partial differential equations. Let the mechanical parameters defining the plate material be its Young's modulus E, its Poisson's ratio v and its density ρ_p. The plate thickness is h and it occupies the segment $]L^-, L^+[$; the abscissae of a point on the plate are denoted by s which varies from ℓ^- to ℓ^+. A condition of free boundaries is assumed. Equation (53a) is replaced by the following system:

$$(\Delta + k^2)p(M) = f(M), \qquad M \in \Omega, \tag{56a}$$

$$\left(\frac{\mathrm{d}^4}{\mathrm{d}s'^4} - \lambda^4\right)u(M') = \mu(M')/D, \qquad M' \in \Sigma, \tag{56b}$$

$$\frac{\partial p}{\partial \mathbf{n}}(M') = \omega^2 \rho_f u(M'), \qquad M' \in \Sigma, \tag{56c}$$

$$u''(M') = 0 = u'''(M') \quad \text{for} \quad M' = L^- \quad \text{or} \quad M' = L^+. \tag{56d}$$

In these equations, λ^4 is defined by $\lambda^4 = \rho_p h \omega^2 / D$, with $D = Eh^3/12(1 - v^2)$ denoting the plate rigidity. The term $\mu = (p^- - p^+)$ represents the difference between the values of the pressure p on the two sides of the screen. The properties of the room boundaries as expressed by equation (53) remain unchanged.

Let $\Gamma(M, M')$ be the Green function of the plate operator in the infinite domain satisfying

$$\left(\frac{\mathrm{d}^4}{\mathrm{d}s'^4} - \lambda^4\right)\Gamma(M', M'') = \frac{1}{D}\,\delta_{M''}(M'), \qquad -\infty \leqslant s' \leqslant +\infty,$$

and a suitable condition at infinity (no incoming waves). One has

$$\Gamma(M', M'') = (\mathrm{e}^{\mathrm{i}\lambda|s'' - s'|} - \mathrm{e}^{-\mathrm{i}\lambda|s'' - s'|})/4\lambda^3 D$$

The Green representation of the plate displacement involves the pressure step μ and a boundary sources vector $\mathbf{S}_u$:

$$u(M') = -\int_\Sigma \mu(M'')\Gamma(M', M'')\,\mathrm{d}s'' + \mathbf{S}_u \cdot \mathscr{G}(M') \qquad \text{on} \quad \Sigma,$$

$$\mathbf{S}_u = \begin{bmatrix} u(L^+) \\ u(L^-) \\ u'(L^+) \\ u'(L^-) \end{bmatrix}, \qquad \mathscr{G} = \begin{bmatrix} D\Gamma'''(P, L^+) \\ D\Gamma'''(P, L^-) \\ D\Gamma''(P, L^+) \\ D\Gamma''(P, L^-) \end{bmatrix}. \tag{57}$$

The choice of the boundary sources is a consequence of the free boundary conditions [4]. The pressure field is again given by equation (54). The continuity condition (56c) leads to the integral equation

$$\frac{\partial p_{in}}{\partial \vec{\mathbf{n}}}(P) - \lim_{P'' \to P} \frac{\partial}{\partial \mathbf{n}} \int_{\Sigma} \mu(P') \frac{\partial G(P'', P')}{\partial \mathbf{n}(P')} \, \mathrm{d}s'$$

$$= \omega^2 \rho_f \left\{ - \int_{\Sigma} \mu(P') \Gamma(P, P') \, \mathrm{d}s' + \mathbf{S}_u \cdot \mathscr{G}(P) \right\} \qquad \text{on} \quad \Sigma. \tag{58}$$

Four additional equations are obtained by applying the boundary conditions (56d) to expression (57).

To get an approximation of the solution $(\mu, \mathbf{S}_u)$, a collocation method is used. The plate domain is divided into N subdomains Σ_i, the length of which is less than one-sixth of both the plate wavelength $2\pi/\lambda$ and the fluid wavelength $2\pi/k$; the function μ is approximated by a piecewise constant function. This approximation is introduced into equation (54) to get the corresponding approximation of the sound pressure field.

4.1.3. *Comparison between the diffraction effects of the rigid screen and of the elastic screen*

The importance of the vibrations of the screen effect appears in equation (58). Indeed, by comparing the two integrals which appear in this expression, it is obvious that the vibrations' effect can be neglected as soon as the operator $\mu \to \omega^2 \rho_f \int \Gamma \mu$ is small compared to the operator $\mu \to \partial_{\mathbf{n}} \int \mu \partial_{\mathbf{n}} G$: that is, if $\omega^2 \rho_f$ is small enough. A refined criterion can be obtained in the particular case of a plane wave impinging on an elastic plate [29]. In the next section, it is shown that the ratio $\rho_f / \rho_p h$ is the coupling parameter which "measures" the influence of the vibrations on the screening effect.

In Figure 12, two configurations of a screen in a room are presented: the first one, in which the screen is above the line source/observation point, corresponds to an idealized two-dimensional concert hall; the second configuration, in which the screen is located between the source and the receiver, is a schematic industrial situation of a protecting screen. A first set of computations have been conducted for the second geometrical configuration of the room (Figure 12 (b)). The screen is either rigid or made of one of the

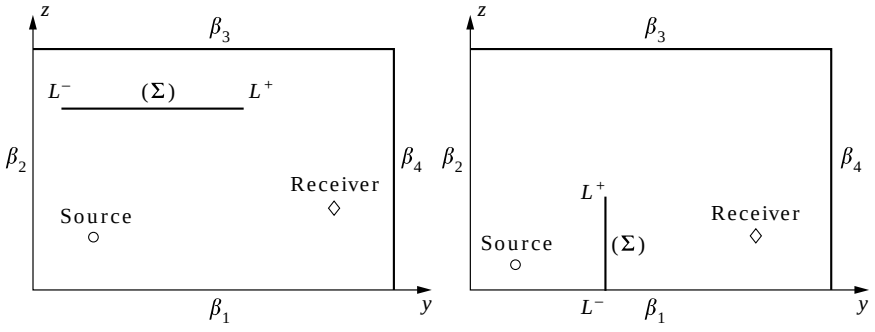

Figure 12. Room geometrical configuration.

TABLE 1

Mechanical data of the screen

Material	ρ_p (kg/m^3)	ν	E (Pa)	h (mm)	f_c (Hz)	λ_c (m)	μ_0/μ (m^{-1})	$\tilde{\mu}_0/\mu$ (λ_c^{-1})
AC	7800	0·28	$2{\cdot}26 \times 10^{11}$	5	2273	0·149	0·033	$0{\cdot}49 \times 10^{-2}$
AG	650	0·30	$4{\cdot}60 \times 10^{9}$	5	4600	0·074	0·397	$2{\cdot}93 \times 10^{-2}$
B	1500	0·28	$2{\cdot}26 \times 10^{11}$	5	991	0·343	0·172	$5{\cdot}90 \times 10^{-2}$

three types of materials defined in Table 1. The room dimensions are 25×9 m^2. The reflection coefficients are 0·8 for the $z = 0$ wall, and 0·7 for the others. The screen length is 3 m; it is normal to the $z = 0$ wall, and extends from $L^- = (12{\cdot}5, 0)$ to $L^+ = (12{\cdot}5, 3)$. The source is isotropic and located at $S = (11{\cdot}5, 0{\cdot}5)$.

The wavelength of the harmonic signal emitted is 6·80 m, the corresponding driving frequency being 50 Hz. The observation line is defined by $13 \text{ m} \leqslant y \leqslant 22 \text{ m}$, $z = 1$ m. Figure 13 shows the excess attenuation: that is, the difference between the sound levels with the screen and without it.

Material AC has the characteristics of steel: large values for both the Young's modulus and the density. Material AG is the lightest, its characteristics are close to those of compressed wood [30]. Material B is in between the Young's modulus of steel and a density 5·2 times less. Far from the screen ($y \geqslant 19$ m), the four curves are very similar. Close to the screen, the differences reach more than 10 dB. The highest attenuation, which is obtained for the steel screen, is of the same order as that given by the perfectly rigid screen. The lowest excess attenuation occurs for the lighest material (material AG). In the last section, other examples are presented.

4.2. APPROXIMATION OF THE SOUND PRESSURE FIELD BY A PERTURBATION METHOD

For an elastic screen, a perturbation method can be adopted as soon as the fluid density is small compared to the surface mass of the structure. Suppose one introduces the

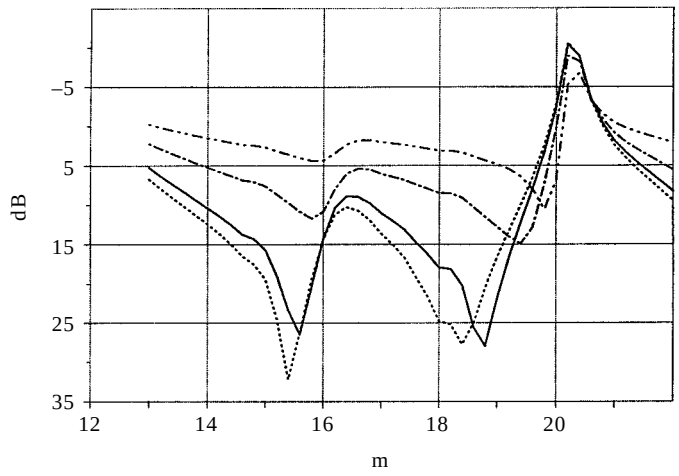

Figure 13. Excess attenuation as a function of the co-ordinate y of the receiver for the second situation (vertical screen); wavelength = 6·80 m, reflection coefficients β; = (0·8, 0·7, 0·7, 0·7). ——, Material AC; – ·–·–·–, material B; ··–··–, material AG; ----, rigid screen.

parameter $\varepsilon = \rho_f/\rho_p h$ which is assumed to be small enough so that the solution $(\mu, \mathbf{S}_u)$ of the boundary integral equations system can be approximated by the first two terms of its Taylor series:

$$\mu = \mu^0 + \varepsilon\mu^1 + \mathcal{O}(\varepsilon^2) \qquad \text{and} \quad \mathbf{S}_u = \mathbf{S}_u^0 + \varepsilon\mathbf{S}_u^1 + \mathcal{O}(\varepsilon^2),$$

where $\mathcal{O}(\varepsilon^2)$ means that the error becomes zero as fast as ε^2. By using the change of unknown function $v = \omega^2\rho_p h u$, the following expansion is introduced:

$$v = v^0 + \varepsilon v^1 + \mathcal{O}(\varepsilon^2).$$

Equations (57) and (58) become

$$\frac{\partial p_{in}}{\partial \mathbf{n}}(M) - \int_\Sigma \mu(P)K(M, P)\,\mathrm{d}\sigma(P) = \varepsilon v(M) \qquad \text{on} \quad \Sigma,$$

$$v(M) = -\int_\Sigma \mu(P)\gamma(M, P)\,\mathrm{d}\sigma(P) + \mathbf{S}_v \cdot \mathscr{G}_\gamma(M) \qquad \text{on} \quad \Sigma, \tag{59}$$

where $\gamma(M, P) = \rho_p h\omega^2\Gamma(M, P)$, $K(M, P) = \partial/\partial\mathbf{n}(M)\partial/\partial\mathbf{n}(P)G(M, P)$ and

$$\mathbf{S}_v \cdot \mathscr{G}_\gamma(M) = \begin{bmatrix} v(L^+) \\ v(L^-) \\ v'(L^+) \\ v'(L^-) \end{bmatrix} \cdot \begin{bmatrix} -D\gamma'''(M, L^+) \\ D\gamma'''(M, L^-) \\ D\gamma''(M, L^+) \\ D\gamma''(M, L^-) \end{bmatrix}.$$

The truncated expansions of μ and $\mathbf{S}_v$ are introduced into equations (59). The zero order terms lead to the following system of equations:

$$\int_\Sigma \mu^0(P)K(M, P)\,\mathrm{d}\sigma(P) = \frac{\partial p_{in}}{\partial \mathbf{n}}(M) \qquad \text{on} \quad \Sigma, \tag{60a}$$

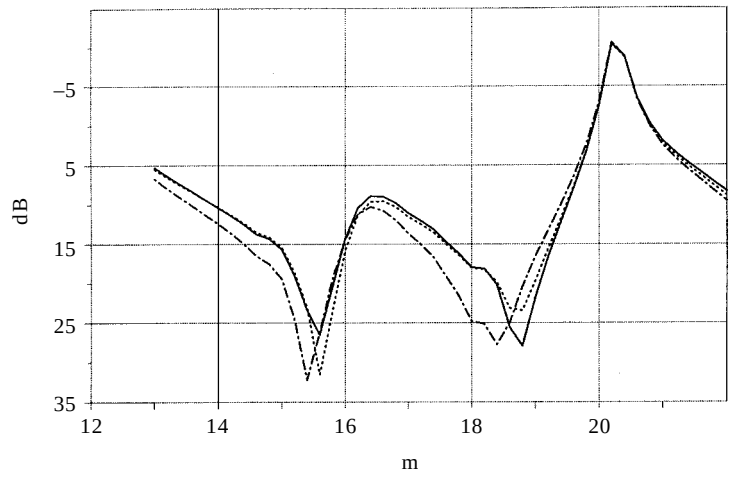

Figure 14. Excess attenuation as a function of the coordinate y of the receiver; vertical screen, material AC, wavelength 6·80 m, reflection coefficients $\beta_j = (0{\cdot}8,\ 0{\cdot}7,\ 0{\cdot}7,\ 0{\cdot}7)$. ——, Exact curve; ·—·—·—, zero order approximation; ---, first order approximation.

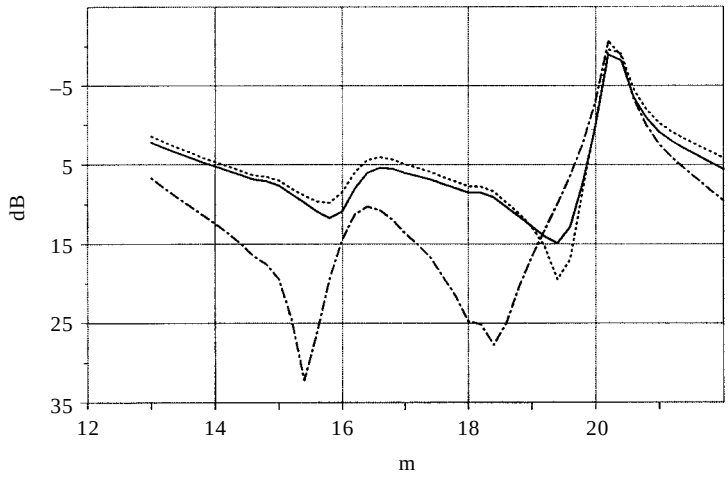

Figure 15. As Figure 14 but for material B.

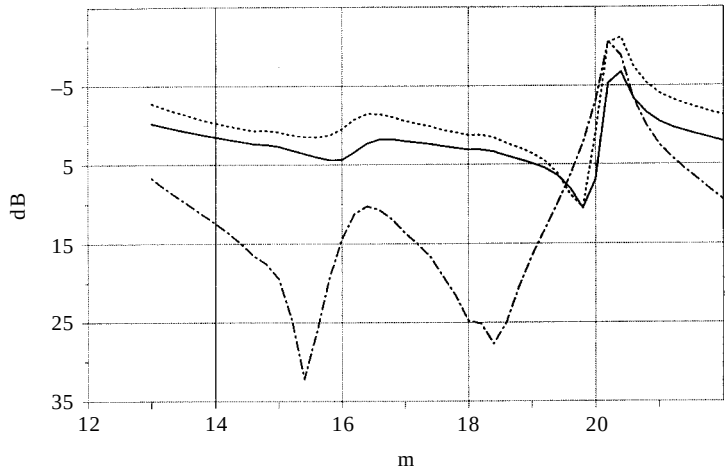

Figure 16. As Figure 14 but for material AG.

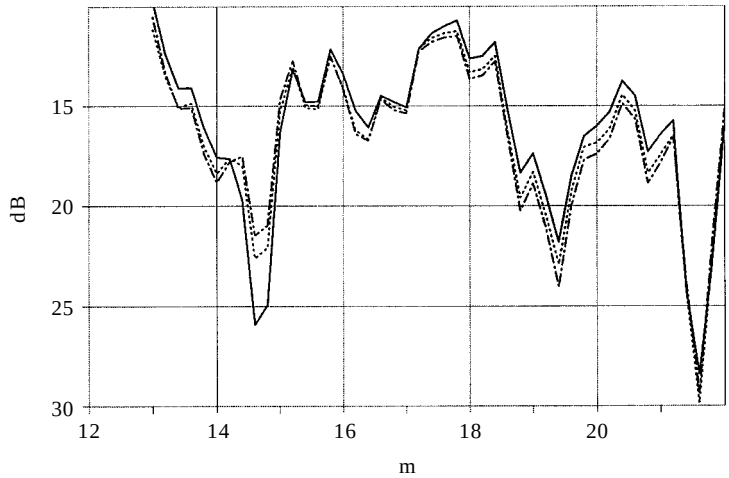

Figure 17. As Figure 14 but for material AC and wavelength 1.36 m.

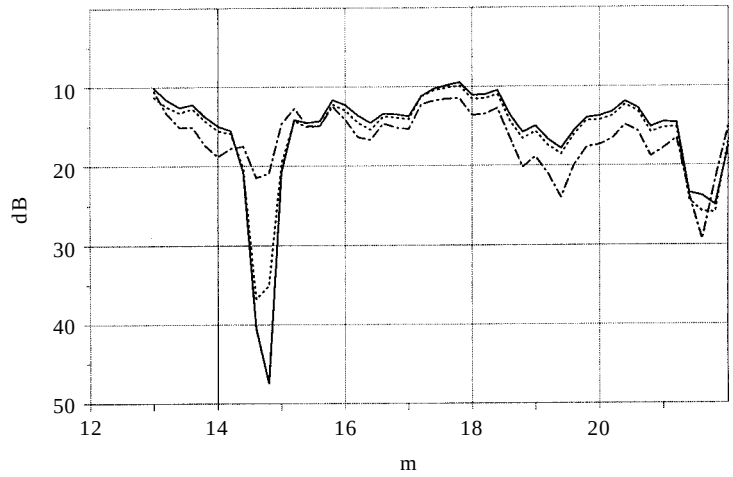

Figure 18. As Figure 15 but wavelength 1·36 m.

$$v^0(M) = -\int_\Sigma \mu^0(P)\gamma(M, P)\,\mathrm{d}\sigma(P) + \mathbf{S}_v^0 \cdot \mathscr{G}_\gamma(M) \qquad \text{on} \quad \Sigma. \tag{60b}$$

The first order term of the first equation (59) leads to

$$-\int_\Sigma \mu^1(P)K(M, P)\,\mathrm{d}\sigma(P) = v^0(M) \qquad \text{on} \quad \Sigma. \tag{61}$$

Equation (60a) corresponds to the perfectly rigid screen. It is solved by a collocation method. Its solution μ^0 is then introduced into expression (60b) and the boundary conditions along the screen boundary provide four algebraic equations to determine the source vector $\mathbf{S}_v^0$. Finally, the zero order approximation of the screen displacement (representation (60b)) is introduced into equation (61).

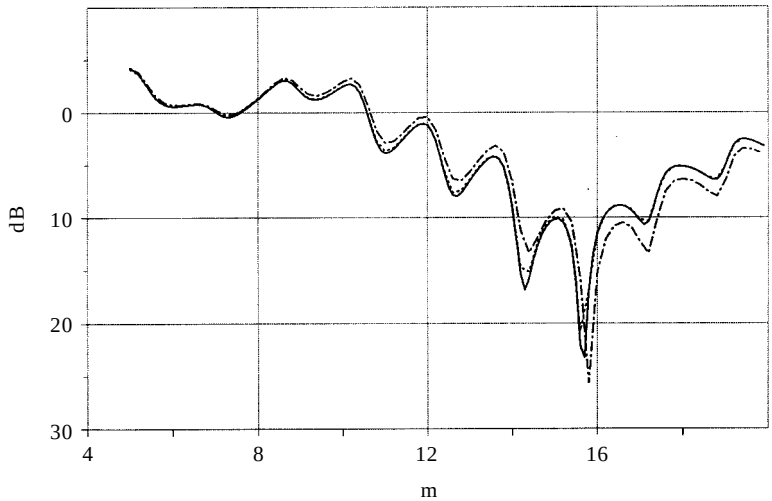

Figure 19. As Figure 14 but wavelength 3·40 m and horizontal screen.

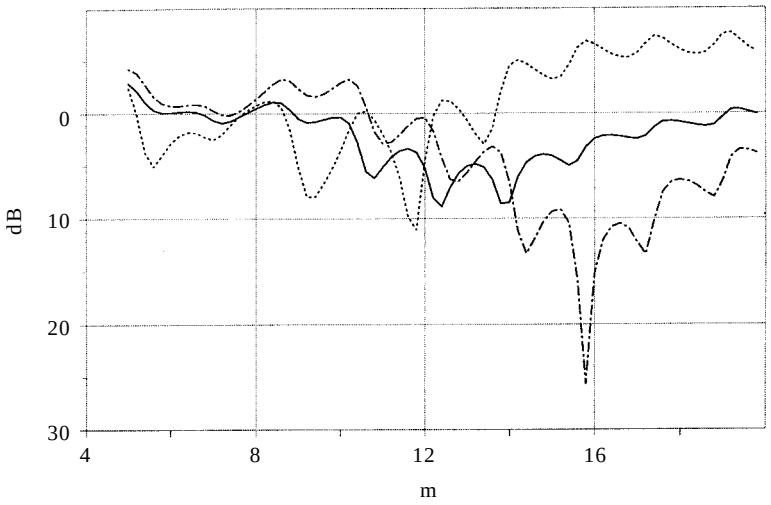

Figure 20. As Figure 16 but wavelength 3·40 m and horizontal screen.

By solving equation (61), the first order correcting term μ^1 of the double layer acoustic source μ is obtained: here again, this equation is that of the perfectly rigid screen. The sound pressure is thus approximated by

$$p(M) \simeq (p^0 + \varepsilon p^1)(M) = p_{in}(M) - \int_\Sigma (\mu^0 + \varepsilon \mu^1)(P) \frac{\partial G(M, P)}{\partial \mathbf{n}(P)} \, \mathrm{d}\sigma(P). \tag{62}$$

This expression accounts partly for the screen vibrations and is a good approximation of the exact solution in so far as the parameter ε is small enough. In the following examples, the meaning of "small enough" will appear clearer.

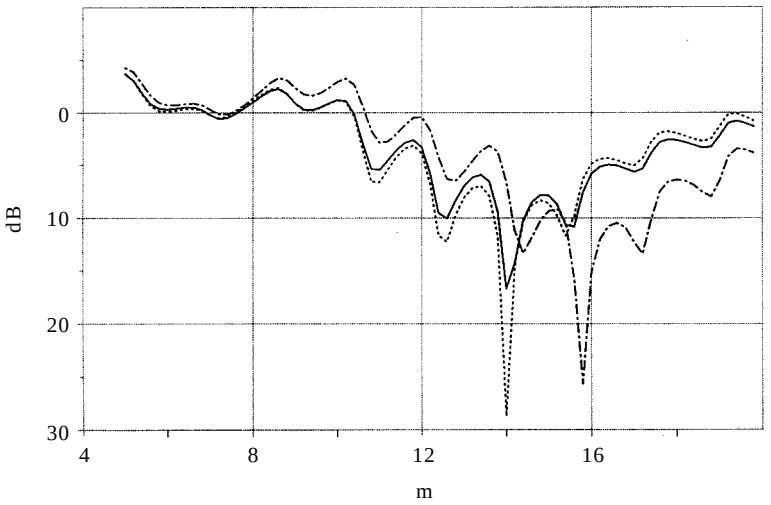

Figure 21. As Figure 15 but wavelength 3·40 m and horizontal screen.

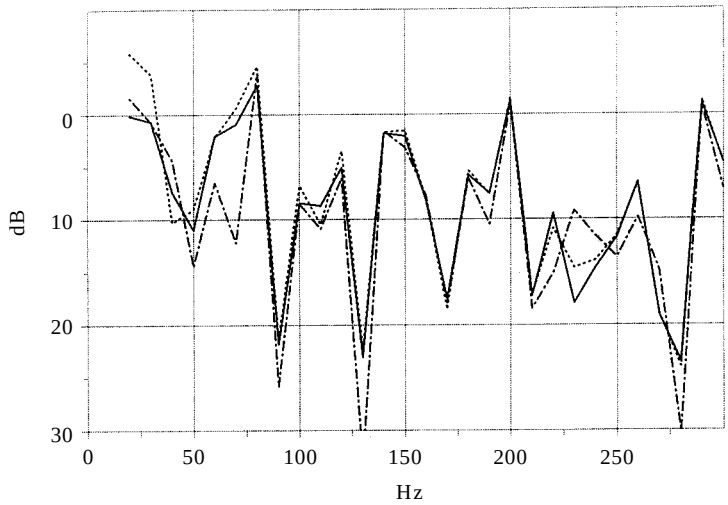

Figure 22. Excess attenuation as a function of the frequency; vertical screen; material B; receiver at (16·0 m, 1·0 m); reflection coefficients $\beta_j = (0{\cdot}8, 0{\cdot}7, 0{\cdot}7, 0{\cdot}7)$——, Exact curve; .–.–, zero order approximation; -----, first order approximation.

4.3. COMPARISON BETWEEN THE FIRST ORDER PERTURBATION APPROXIMATION AND THE NUMERICAL SOLUTION OF THE EXACT EQUATIONS

Here the geometries defined in section 4.1.2 and the screen characteristics given in Table 1 are considered. It has been seen in section 4.1.3 that the elasticity of the screen is important mainly at low frequencies and for low screen density; in other circumstances, the screen is correctly described as a perfectly rigid infinitely thin diffracting object.

The dimensions of the room are $(0{\cdot}0\text{ m} \leqslant y \leqslant 25{\cdot}0\text{ m};\ 0{\cdot}0\text{ m} \leqslant z \leqslant 9{\cdot}0\text{ m})$. For the configuration of Figure 12(a), the screen, which is in a "horizontal" position, extends from $L^- = (2{\cdot}5\text{ m},\ 5{\cdot}0\text{ m})$ to $L^+ = (10{\cdot}0\text{ m},\ 5{\cdot}0\text{ m})$. A point isotropic source is located at $S = (1{\cdot}25\text{ m},\ 2{\cdot}0\text{ m})$ and the sound field is calculated along the line $(13{\cdot}0\text{ m} \leqslant y \leqslant 23{\cdot}0\text{ m},\ z = 1{\cdot}0\text{ m})$.

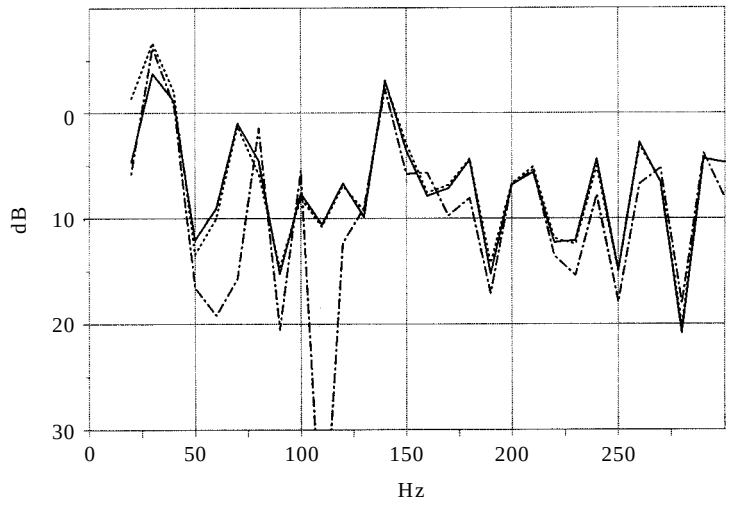

Figure 23. As Figure 22 but receiver at (19·0 m, 1·0 m).

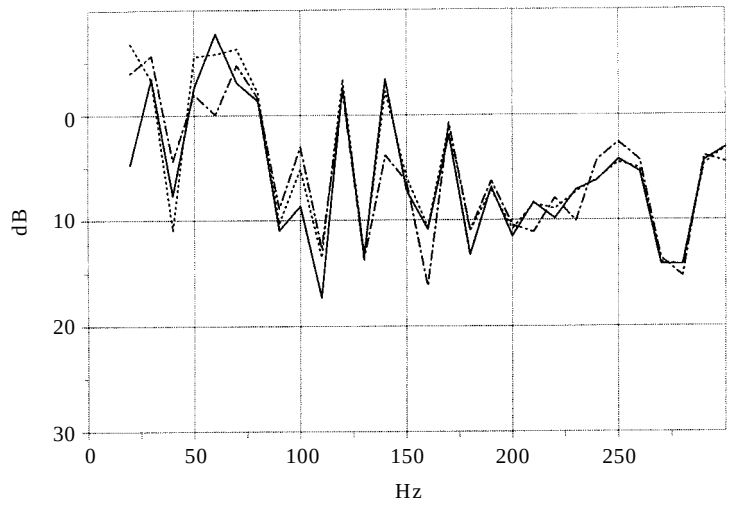

Figure 24. As Figure 22 but receiver at (13·0 m, 1·0 m), and reflection coefficients $\beta_j = (0{\cdot}0, 0{\cdot}9, 0{\cdot}9, 0{\cdot}9)$.

For the configuration of Figure 12(b), the screen, which is in a "vertical" position, extends from $L^- = (12{\cdot}5\text{ m},\ 0{\cdot}0\text{ m})$ to $L^+ = (12{\cdot}5\text{ m},\ 3\text{ m})$. A point isotropic source is located at $S = (11{\cdot}5\text{ m},\ 0{\cdot}5\text{ m})$ and the sound field is calculated along the line $(13{\cdot}0\text{ m} \leqslant y \leqslant 23{\cdot}0\text{ m},\ z = 1{\cdot}0\text{ m})$.

The results present the excess attentuation obtained in the presence of the screen: that is the difference between the sound pressure levels with and without the screen. Two sets of curves have been calculated: in the first set, the driving frequency is fixed and the observation point position is varied, while in the second set the observation point is fixed and the frequency is varied.

Figures 14–25 present the excess attenuation as a function of the receiver position for a fixed frequency. For Figures 14–16, the screen is perpendicular to the y-axis (vertical position), the frequency is 50 Hz (wavelength = 6·80 m) and the reflection coefficients are $\beta_j = (0{\cdot}8, 0{\cdot}7, 0{\cdot}7, 0{\cdot}7)$. They provide a good test of the efficiency of the perturbation

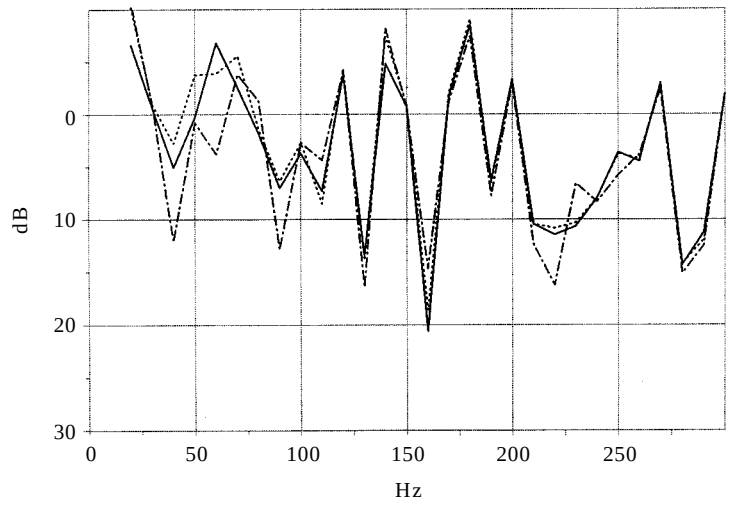

Figure 25. As Figure 24 but receiver at (16·0 m, 1·0 m).

method. For material AC ($\varepsilon = 0{\cdot}033$), the difference between the zero order approximation (perfectly rigid screen) of the excess attentuation and the exact one (vibrating plate) is small, and the first order approximation gives an almost perfect result. For materials B ($\varepsilon = 0{\cdot}17$) and AG ($\varepsilon = 0{\cdot}40$), the difference between the zero order approximation and the exact curve is much larger: nevertheless, the correction given by the first order approximation is still good enough.

Figures 17 and 18 correspond to a higher frequency (250 Hz, wavelength = 1·36 m) and lower reflection coefficients $\beta_j = (0{\cdot}8, 0{\cdot}3, 0{\cdot}3, 0{\cdot}3)$. With these data, the difference between the excess attenuation due to the perfectly rigid screen and that due to the steel one (material AC) is no more significant. For material B, the difference between the perfectly rigid screen remains important and the first order approximation provides the necessary correction.

Figures 19–21 were obtained for a horizontal screen, with a driving frequency equal to 100 Hz (wavelength = 3·40 m) and the following set of reflection coefficients $\beta_j = (0{\cdot}8, 0{\cdot}3, 0{\cdot}3, 0{\cdot}3)$. For material AC, the difference between the excess attenuation due to the perfectly rigid screen and that provided by the elastic plate is not significant. This result is quite reasonable: indeed, in this situation, the source and the receiver are both on the same side of the diffracting obstable and both far away from it, thus reducing its influence. For material AG, the difference remains important due to the fact that a light screen is more easily excited by the incident acoustic wave. The first order approximation provides a correction which is not really bad, but is not sufficient due to the fact that the parameter ϵ is too large.

In Figures 22–25 the excess attenuation is presented as a function of the frequency over a range 20–300 Hz for a given position of the receiver; the configuration of a vertical screen has been adopted and the screen is made of material B. As has been mentioned in section 4.1.3, the difference between the rigid screen and the elastic one must decrease as the frequency is increased. This general tendency is confirmed by all the results presented here. The first two sets of curves (Figures 22 and 23) correspond to reflection coefficients $\beta_j = (0{\cdot}8, 0{\cdot}7, 0{\cdot}7, 0{\cdot}7)$ and two receiver positions $M = (16{\cdot}0\text{ m}, 1{\cdot}0\text{ m})$ and $M = (19{\cdot}0\text{ m}, 1{\cdot}0\text{ m})$. The other two (Figures 24 and 25) are for the reflection coefficients $\beta_j = (0, 0{\cdot}9, 0{\cdot}9, 0{\cdot}9)$ and the receiver positions $M = (13{\cdot}0\text{ m}, 1{\cdot}0\text{ m})$ and $M = (16{\cdot}0\text{ m}, 1{\cdot}0\text{ m})$. In both cases, the first order approximation gives a prediction of the excess attenuation with an accuracy which is not dependent on the boundary conditions on the room walls.

For all the configurations studied it appears that the perturbation method is a powerful tool: its accuracy is quite sufficient when the parameter ϵ is less than 0·2; furthermore, the computation time is about three times less than that required by solving the coupled system of boundary integral equations.

5. CONCLUSION

Several canonical problems of vibro-acoustics have been presented in which a thin elastic structure is coupled to a gas. Because of the low density of the fluid, the fluid/structure coupling is weak and a perturbation method can be used: the small parameter which is involved is the ratio of the gas density to the structure surface mass.

Three examples have been developed which show the efficiency of such methods, and two different approaches have been considered.

In the first one, the structure displacement is expanded into a series of the fluid-loaded modes of the structure, instead of in the *in vacuo* modes which are more classically used; then, a small parameter method is developed to get an approximation to these fluid-loaded modes in terms of the *in vacuo* ones. As a consequence, the structure displacement is

expressed as a series of the *in vacuo* modes. The same final series can be obtained directly by looking at the structure displacement as a series of the resonance modes of the "dry" elastic solid: one is left with an infinite system of algebraic equations; solving it by a perturbation method leads to the results that have been given here. But, the resonance frequencies of the fluid-loaded structure cannot be identified as easily and the expression for the perturbed resonance régimes are not obtained.

In the second approach, a global representation of the system response by boundary integrals is adopted. The boundary integral equations thus derived are solved by a perturbation technique applied to a classical boundary element method.

This type of perturbation algorithms, which has been developed here for two particular classical methods, apply for any other numerical approximation. Two basic computation programmes are required: one which solves the vibration problem of the *in vacuo* structure; and another one which solves the diffraction problem by a perfectly rigid body (Neumann boundary condition). The perturbation method consists of an iterative procedure in which a structure problem and a diffraction problem are alternatively solved at each step.

The examples which have been presented show clearly that the accuracy of the result is independent of the basic method—modal expansion or global representation—which is adopted. Nevertheless, depending on the results which are desired, a particular representation of the solution can be chosen. A perturbation calculation based on a boundary element method is very suitable when the objective is to establish a sound pressure level chart for a given set of isolated frequencies. Conversely, if a broad frequency bandwidth excitation (transient signal, randomly time-dependent sources, . . .) is involved, a resonance modes expansion representation of the solution seems to be the most convenient. To compute the resonance frequencies and the resonance modes, any numerical method which solves the *in vacuo* structure problem and the diffraction problem can be used: in particular, a perturbation algorithm based on a boundary element method is efficient.

As a final remark, let us recall that the method which has been presented for the particular example of a thin plate applies to any kind of structure immersed in a *light* fluid. For example, in reference [31], the authors applied this technique to a more complex structure: a bounded cylindrical thin shell, extended by two semi-infinite perfectly rigid cylinders, embedded in air and excited by an internal turbulent air flow (an additional difficulty appears due to the cut-off frequencies of the cylindrical wave guide). In general, the fluid-loaded structure can have resonance modes which do not radiate acoustic energy: they are the structure modes which correspond to purely tangential displacement of the surface of the elastic solid in contact with the fluid. Though such modes belong to the set of resonance modes of the coupled system, they must be skipped from the representation of the solution of the fluid/structure interaction problem. But the consequence is that the uniqueness of the solution of the coupled equations is not ensured in the general case, and this implies numerical instabilities which require some care.

ACKNOWLEDGMENT

This research has been partly sponsored by the Ministère de l'Environnement and by the Programme International de Coopération Scientifique *Vibro-Acoustique dans le Domaine des Transports* initiated by the C.N.R.S.

REFERENCES

1. P. J. T. Filippi, O. Lagarrigue and P.-O. Mattei 1994 *Journal of Sound and Vibration* **177**, 259–275. Perturbation method for sound radiation by a vibrating plate in a light fluid: comparison with the exact solution.

2. C. Bardos, M. Concordel and G. Lebeau 1989 *Journal d'Acoustique* **2**, 31–38. Extension de la théorie de la diffusion pour un corps élastique immergé dans un fluide. Comportement asymptotique des résonances.
3. Ph. Morse and K. U. Ingard 1968 *Theoretical Acoustics*. New York: McGraw-Hill Book Company.
4. J. Vivoli and P. Filippi 1974 *Journal of the Acoustical Society of America* **55**, 562–567. Eigenfrequencies of thin plates and layer potentials.
5. P. J. T. Filippi 1988 in *Boundary Elements X* Boundary elements methods in acoustics and vibrations: a review of the last twenty years. (volume 4) (C. A. Brebbia, editor), 269–287. Berlin: Springer-Verlag.
6. D. G. Crighton 1989 *Journal of Sound and Vibration* **133**, 1–27. The 1988 Rayleigh medal lecture: fluid loading—the interaction between sound and vibration.
7. P. M. Morse and H. Feshbach 1953 *Methods of Theoretical Physics*. New York: McGraw-Hill Book Company.
8. R. Courant and D. Hilbert 1957 *Methods of Mathematical Physics*. New York: Interscience.
9. A. Nayfeh. *Perturbation Methods* 1973. John Wiley and Sons.
10. P. J. T. Filippi and P.-O. Mattei 1992 in *Boundary Elements XIV* (volume 1) (F. Paris, C. A. Brebbia and J. Dominguez, editors), 279–291. Sound radiation by a thin baffled plate embedded in a 'light'' fluid: boundary integral equations deduced from a perturbation method. Southampton-Boston and London-New York: Computational Mechanics Publications and Elsevier Science Publishers.
11. P. J. T. Filippi and D. Mazzoni 1994 in *Boundary Elements XVI* (C. A. Brebbia, editor), 47–54. Noise induced inside a cavity by an external turbulent boundary layer. Southampton-Boston: Computational Mechanics Publications.
12. M. B. Priestley 1989 *Spectral Analysis and Time Series*. London: Academic Press.
13. G. M. Corcos 1963 *Journal of the Acoustical Society of America* **35**, 192–199. Resolution of pressure in turbulence.
14. D. M. Chase 1990 *Journal of the Acoustical Society of America* **90**, 1032–1034. The wave–vector -frequency spectrum of pressure on a smooth plane in turbulent boundary layer flow at low Mach number.
15. A. Norris, G. A. Kriegsmann and E. L. Reiss 1984 *Journal of the Acoustical Society of America* **75**, 685–694. Acoustic scattering by baffled membranes.
16. A. Norris 1990 *Journal of the Acoustical Society of America* **88**, 505–514. Resonant acoustic scattering from solid targets.
17. N. C. Martin and P. Leehey 1977 *Journal of Sound and Vibration* **52**, 95–120. Low wavenumber wall pressure measurements using a rectangular membrane as a spatial filter.
18. H. G. Davies 1969 *Journal of the Acoustical Society of America* **49**, 878–889. Sound from turbulent-boundary-layer-excited panels.
19. L. Jourdan, J.-P. Guibergia, S. Bano and R. Marmey 1992 *Journal d'Acoustique* **5**, 99–124. Etude théorique et expérimentale de la réponse vibroacoustique d'une plaque couplée à une cavité en fluide lourd.
20. M. L. Rumerman 1992 *Journal of the Acoustical Society of America* **91**, 907–910. Frequency-flow speed dependence of structural response to turbulent boundary layer excitation of a panel.
21. M. S. Howe 1988 *Journal of Sound and Vibration* **121**, 47–65. Diffraction radiation produced by turbulent boundary layer excitation of a panel.
22. M. S. Howe 1988 *Journal of Sound and Vibration* **144**, 229–245. Sound and vibration produced by an airfoil tip in boundary layer flow over an elastic plate.
23. P. L. Shah and M. S. Howe 1996 *Journal of Sound and Vibration* **197**, 103–115. Sound generated by a vortex interacting with a rib-stiffened elastic plate.
24. M. S. Howe and P. L. Shah 1996 *Journal of the Acoustical Society of America* **99**, 3401–3411. Influence of mean flow on boundary layer generated interior noise.
25. P. J. T. Filippi 1997 *Journal of Sound and Vibration* **54**, 473–500. Layer potentials and acoustic diffraction.
26. A. Daumas 1978 *Acustica* **40**, 213–222. Etude de la diffraction par un écran mince disposé sur le sol.
27. M. N. Sayhi, Y. Ousset and G. Verchery 1981 *Journal of Sound and Vibration* **74**, 187–204. Solutions of radiation problems by collocation of integral formulations in terms of single and double layer potentials.
28. J. B. Allen and D. A. Berkley 1979 *Journal of the Acoustical Society of America* **65**, 943–950. Image method for efficiently simulating small-room acoustics.

29. C. LESUEUR 1988 *Rayonnement Acoustique des Structures*. Paris: Eyrolles, Collection de la Direction des Etudes et Recherches d'Electricité de France.
30. F. J. FAHY 1985 *Sound and Structural Vibration* London: Academic Press.
31. P.-O. MATTEI and P. J. T. FILIPPI 1997 in *Euromech 369—Fluid/Structure Interactions in Acoustics*, Delft 23–26 1997. Response of a thin cylindrical shell excited by a turbulent internal flow.